Boletín Sociedad Entomológica Aragonesa, nº **43** (2008) : 255–281.

CLADISTIC ANALYSIS OF SUPERFAMILY IUROIDEA, WITH EMPHASIS ON SUBFAMILY HADRURINAE (SCORPIONES: IURIDA)

Victor Fet [1] & Michael E. Soleglad [2]

[1] Department of Biological Sciences, Marshall University, Huntington, WV 25755-2510, USA
[2] P. O. Box 250, Borrego Springs, California 92004, USA

Abstract: A detailed cladistic analysis of the scorpion superfamily Iuroidea, with special emphasis on the subfamily Hadrurinae (family Caraboctonidae), is presented. This study follows a layered approach to cladistic analysis, with fundamental (higher-level) characters analyzed first. Included in this analysis is a critical review of the recent study by Francke & Prendini (2008). Based on the outcome of our cladistic analysis, we demonstrate that the main result of Francke & Prendini (2008), a phylogeny leading to synonymization of *Hoffmannihadrurus* Fet et Soleglad, 2004 in Fet *et al.* (2004), is not supported. Consequently, *Hoffmannihadrurus* is reinstated as a genus: *Hadrurus aztecus* Pocock, 1902 = *Hoffmannihadrurus aztecus* (Pocock, 1902), **comb. nov.**; *Hadrurus gertschi* Soleglad, 1976 = *Hoffmannihadrurus gertschi* (Soleglad, 1976), **comb. nov.** We also present a biogeographic discussion and a distribution map of the subfamily Hadrurinae.
Key words: Scorpiones, Iuroidea, Iuridae, Caraboctonidae, Caraboctoninae, Hadrurinae, *Hoffmannihadrurus aztecus* **comb. nov.**, *Hoffmannihadrurus gertschi* **comb. nov.**, cladistics, biogeography.

Análisis cladístico de la superfamilia Iuroidea, con énfasis en la subfamilia Hadrurinae (Scorpiones: Iurida)
Resumen: Se presenta un análisis cladístico detallado de la superfamilia Iuroidea, con énfasis especial en la subfamilia Hadrurinae (familia Caraboctonidae). El estudio se basa en un análisis de capas que parte de los caracteres fundamentales (de más alto nivel). En el análisis se incluye una revisión crítica del reciente trabajo de Francke & Prendini (2008). El resultado de nuestro análisis cladístico no respalda el resultado principal de Francke & Prendini (2008), una filogenia que les llevaba a sinonimizar *Hoffmannihadrurus* Fet et Soleglad, 2004 in Fet *et al*. (2004), is not supported. En consecuencia, *Hoffmannihadrurus* se restablece como género: *Hadrurus aztecus* Pocock, 1902 = *Hoffmannihadrurus aztecus* (Pocock, 1902), **comb. nov.**; *Hadrurus gertschi* Soleglad, 1976 = *Hoffmannihadrurus gertschi* (Soleglad, 1976), **comb. nov.** También presentamos una discusión biogeográfica y un mapa de distribución de la subfamilia Hadrurinae.
Palabras clave: Scorpiones, Iuroidea, Iuridae, Caraboctonidae, Caraboctoninae, Hadrurinae, *Hoffmannihadrurus aztecus* **comb. nov.**, *Hoffmannihadrurus gertschi* **comb. nov.**, cladística, biogeografía.

Introduction

The history of the systematic study of scorpion superfamily Iuroidea, its phylogenetic analysis, and important morphology of this family were presented by Soleglad & Fet (2003b) in the context of general phylogenetic analysis of orthostern scorpions. Following the family-group classification of Soleglad & Fet (2003b), we include in Iuroidea two families: the Old World family Iuridae (with genera *Iurus* Thorell, 1876 and *Calchas* Birula, 1899) and the New World family Caraboctonidae. The family Caraboctonidae includes South American subfamily Caraboctoninae (with genera *Caraboctonus* Pocock, 1893 and *Hadruroides* Pocock, 1893) and North American subfamily Hadrurinae (with genera *Hadrurus* Thorell, 1876 and *Hoffmannihadrurus* Fet et Soleglad, 2004). Additional information on systematics, morphology, and phylogeny of the North American genus *Hadrurus* can be found in the works of Stahnke (1945, 1969, 1971), Williams (1970a, 1970b), Soleglad (1976), Fet *et al*. (2001, 2004), and Francke & Prendini (2008). For pre-1998 taxonomic details, taxonomic history and references, as well as the full species list of Iuroidea, see Sissom & Fet (2000) under family Iuridae.

Prendini & Wheeler (2005), without presenting any specific new data or their own analyses, severely criticized the cladistic approach of Soleglad & Fet (2003b), reversed all changes in scorpion taxonomy introduced in Soleglad & Fet (2003b) and in several other works of these authors and their associates. Among other nomenclatural acts, Prendini & Wheeler (2005) synonymized the genus *Hoffmannihadrurus* Fet et Soleglad, 2004 (described in Fet *et al*., 2004). Fet & Soleglad (2005) rejected all changes of Prendini & Wheeler (2005) as unjustified, and reversed their synonymizations.

Most recently, Francke & Prendini (2008) published a "reappraisal" based on the examination of impressive material, the total of 245 specimens, among them 69 specimens for outgroups (including 37 for *Caraboctonus* and *Hadruroides*) and 176 specimens for *Hadrurus* (including *Hoffmannihadrurus*); see their Appendix 2. As the result of their cladistic analysis, Francke & Prendini (2008) obtained a phylogeny that did not support monophyly of *Hoffmannihadrurus*, and again formally synonymized genus *Hoffmannihadrurus* with *Hadrurus*.

It is interesting to note that Francke & Prendini (2008), in their detailed taxonomic history, preferred not to mention at all two important nomenclatural acts: that Prendini & Wheeler (2005) already once synonymized *Hoffmannihadrurus*, without any specific analysis or justification; and that Fet & Soleglad (2005) restored it from this unjustified synonymy.

Another minor observation is that Francke & Prendini (2008) consistently misquote the authorship of *Hoffmannihadrurus* as "Fet *et al*., 2004". The authors of this generic name, as clearly stated in Fet *et al*. (2004), are Fet and Soleglad only, not all four authors of the Fet *et al*. (2004) pa-

per (David Neff and Iasmi Stathi contributed valuable research effort but are not the coauthors of the new generic name). Such an arrangement, while rare, is traditionally used in systematics; the full reference, if needed, should be cited as "Fet et Soleglad in Fet *et al*., 2004." Attention to such nomenclatural details is important, since exact authorship assigns responsibility. For example, since it was not stated otherwise, both Prendini and Wheeler (2005) were responsible for multiple, unjustified nomenclatural acts in their wholesale reversal of changes proposed by Soleglad and Fet (but not other authors) at any time after 2003—whether those changes resulted from formal cladistic analyses or not.

The decision of Soleglad and Fet (in Fet *et al*., 2004) to establish the genus *Hoffmannihadrurus* was based on a few solid characters, but has not been a result of a formal cladistic analysis. Such analysis was conducted by Francke & Prendini (2008), who did not recover the monophyly of genus *Hoffmannihadrurus*—first rejected by Prendini & Wheeler (2005) without any justification whatsoever. Therefore, one would be interested to see what justification is now presented by Francke & Prendini (2008) for a phylogeny that again results in the same generic synonymy—the only taxonomic change given in their "reappraisal".

In this paper, we first evaluate the reappraisal of Hadrurinae conducted by Francke & Prendini (2008). We examine in detail the claimed robustness of their analysis and stated result, as well as individual character analysis, their interpretations and assumed homologies. We show in detail that Francke & Prendini's (2008) result is not as robust as suggested by these authors. Furthermore, we reject most of their character analysis interpretations and subsequent homology assumptions. Some of our objections are not only with interpretations of characters but with actual inaccuracies in Francke & Prendini's analysis, which we corroborate by the examination of material. Based on our analysis of Francke & Prendini's results, in conjunction with the new phylogenetic analysis presented herein, their phylogeny is rejected. The genus *Hoffmannihadrurus*, monophyly of which is confirmed by our cladistic analysis, is reinstated.

In our cladistic analysis of morphological characters, three separate, successive analytic sequences are presented that include analysis of: (a) fundamental characters—characters that, in general, are germane to higher phylogenetic levels such as parvorders, superfamilies, subfamilies, genera. These characters, which comprised over 70 % of the characters, are non-ordered, equal-weighted, and hypothesis-free; (b) low-level characters, such as coloration and its patterns, setation, which typically are generic or intrageneric in level, are added to the fundamental characters; and (c) the accessory trichobothria loss hypothesis presented by Soleglad & Fet (2004) is modeled with cladistic characters and added to sequence (b), completing our final result. Incidentally, all three cladistic sequences outlined above support the monophyly of genus *Hoffmannihadrurus*. Each successive analysis further delineates the finer topology of the obtained phylogeny of subfamily Hadrurinae.

Following the cladistic analysis of morphological characters, we present a discussion of the geographical distribution of subfamily Hadrurinae, accompanied with a map depicting the distribution of its species. A simple biogeographic model is presented and analyzed cladistically, independently of morphology. This simple model is congruent with our phylogenetic result based on morphology. Interestingly, the phylogeny presented in this paper is consistent with a classification scheme suggested by Stanley C. Williams (1970b) nearly 40 years ago.

Nomenclatural changes

Hoffmannihadrurus Fet et Soleglad, 2004 is here reinstated as a genus. It comprises two species: *Hadrurus aztecus* Pocock, 1902 = *Hoffmannihadrurus aztecus* (Pocock, 1902) **comb. nov.,** and *Hadrurus gertschi* Soleglad, 1976 = *Hoffmannihadrurus gertschi* (Soleglad, 1976), **comb. nov.**

In the remainder of this paper, we use the taxonomic nomenclature established in this paper, including any formal emendations. See below on the status of the subspecies *Hadrurus arizonensis pallidus* Williams, 1970, which remains in synonymy with the nominotypical subspecies *Hadrurus arizonensis arizonensis* Ewing, 1928 as synonymized by Fet *et al.* (2001).

Methods & Material

Cladistic analysis software packages

Software package PAUP* Version 4 (Beta) (Swofford, 1998) was used for Maximum Parsimony (MP) analysis of character codings producing results of tree searches, implied and successive weighting, consensus trees, and bootstrap and jackknife resampling sequences. TreeView (Win 32) Version 1.5.2 (Page, 1998) and Winclada Version 0.9.3 (Nixon, 1999) were used, in part, to generate the resulting PAUP* cladograms showing clade support and distribution of all characters and their states as augmented with the Metafile Companion editor, Version 1.11 (Companion Software, Inc.).

Abbreviations

List of depositories: CAS, California Academy of Sciences, San Francisco, California, USA; FK, Personal collection of František Kovařík, Prague, Czech Republic; MES, Personal collection of Michael E. Soleglad, Borrego Springs, California, USA; MRG, Personal collection of Matthew R. Graham, Las Vegas, Nevada, USA. NMW, Naturhistorisches Museum, Vienna, Austria; VF, Personal collection of Victor Fet, Huntington, West Virginia, USA.

Other: ABDSP, Anza-Borrego Desert State Park, San Diego and Riverside Counties, California, USA.

Material examined

The following chaeriloid and iuroid material was examined for analysis and/or illustrations provided in this paper. The list of material reflects the taxonomic changes established in this paper.

***Parvorder Chaerilida: Chaeriloidea, Chaerilidae*:**
Chaerilus variegatus Simon, 1877, Indonesia, ♂ (MES).

Parvorder Iurida: Iuroidea:
● **Iuridae:**
Calchas nordmanni Birula, 1899, Baykan, Turkey, ♀ (NMW), Anamur, Turkey, ♂ ♀ (NMW); *Iurus dufoureuis* (Brullé, 1832), Gythio, Greece, ♂ (VF), Turkey, ♀ (MES), Antalya, Turkey, ♂ ♀ (FK).

• **Caraboctonidae:**
Caraboctonus keyserlingi Pocock, 1893, Chile, ♂ (MES); *Hadruroides charcasus* (Karsch, 1879), Peru, ♂ (MES); *Hadruroides maculatus* (Thorell, 1876), Huancayo, Peru, 3 ♂ 12 ♀ (MES); *Hoffmannihadrurus aztecus* (Pocock, 1902), Tomellín, Oaxaca, Mexico, ♂ (MES), Tehuacán, Puebla, Mexico, 5 ♂ ♀ (MES); *Hoffmannihadrurus gertschi* (Soleglad, 1976), Iguala, Guerrero, Mexico, ♀ (MES), Azcala, Guerrero, Mexico, paratype ♀ (CAS); *Hadrurus arizonensis arizonensis* Ewing, 1928, Carrizo Badlands, ABDSP, California, USA, ♂ (MES); *Hadrurus arizonensis austrinus* Williams, 1970, Oakies Landing, Baja California, Mexico, ♂ ♀ (MES); *Hadrurus concolorous* Stahnke, 1969, Santa Rosalia, Baja California Sur, Mexico, 2 ♂ ♀ (MES); *Hadrurus hirsutus* (Wood, 1863), Cabo San Lucas, Baja California Sur, Mexico, 2 ♂ (MES); *Hadrurus obscurus* Williams, 1970, Pinyon Mountain, ABDSP, California, USA, ♂ ♀ (MES), Indian Gorge Canyon, ABDSP, California, USA, 2 ♀ (MES); *Hadrurus pinteri* Stahnke, 1969, Oakies Landing, Baja California, Mexico, ♂ 2 ♀ (MES), Loreto, Baja California Sur, Mexico, ♂ (CAS), San Miguel de Comondú, Baja California Sur, Mexico, 2 ♂ (CAS), Isla Danzante, Baja California Sur, Mexico, 3 ♀ (CAS); *Hadrurus spadix* Stahnke, 1940, Winnemucca, Humboldt Co., Nevada, USA, ♂ ♀ (MRG).

Examination of Francke & Prendini (2008) results

Initial observations and analysis. Francke & Prendini (2008) state in their abstract: "… Seven independent analyses of the morphological character matrix, under weighting regimes that minimised length as well as those that maximised fit, each located a single most parsimonious tree …" This impressive statement certainly implies a very robust result, a result that is supported by no less than seven "independent analyses". The authors also state (p. 213) "…The most *surprising* (our italics) result of our reanalysis is the close phylogenetic relationship between *H. gertschi* and *H. pinteri*, …" We now examine the robustness of this result.

First, with respect to seven "independent analyses", six of these analyses involved implied weighting, an algorithm that minimizes the effect of homoplasious characters (see Goloboff, 1993). The minimizing aspect of this algorithm is controlled by six concavity index values, resulting in six "independent analyses", the seventh being the analysis where homoplasy impact was not controlled (i.e., equal weighting). We need to point out here that the homoplasy index of Francke & Prendini's (2008) result is somewhat small, a 0.29 (i.e., they report a consistency index of 0.71 percent, see their table 5). We suggest here that one would not necessarily obtain a different result from implied weight analysis with this limited homoplasy and a rather small number of informative characters (only 32), and certainly not from the larger concavity index values (i.e., larger values impact homoplasy the least). In support of this observation, we note that Soleglad & Sissom (2001: 82), in their cladistic revision of family Euscorpiidae, state the following: "… The overall homoplasy of this analysis was relatively small, having a homoplasy index of 0.1542 (i.e. 1 - CI). Consequently, any attempt to generate alternative topologies by a *posteriori* weighting techniques using either successive weights (the REWEIGHT command in PAUP*) or implied weights (the GOLOBOFF mode in PAUP*) was unsuccessful." We might add here that our results, presented elsewhere in this paper, and based on an entirely different set of characters, were also not impacted by exercising all six implied weighting sequences as well as Farris' successive weighting algorithm. Therefore, as Francke & Prendini (2008), we could say that our result was supported by no less than eight "independent analyses". It is important to note that Prendini (2000: figs. 3c–f; 2003: tab. 1), in his scorpionoid and bothriurid revisions, derived different results from implied weighting sequences (in fact, all were different in the former, and two out of six in the latter). In this case the homoplasy indices were somewhat large, 0.45 (CI = 0.55) and 0.37 (CI = 0.63) percent, respectively. As can be seen in these data, the analysis with the most homoplasy, a CI of 0.55, was more affected by implied weighting than the other, a CI of 0.63. Unfortunately, however, in the end Prendini (2000) decided the result based on equal weights and ordered characters was the "best explanation" of the data, and completely ignored the implied weighting results. Soleglad *et al*. (2005) showed in great detail that the implied weighting result illustrated in Prendini's (2000) figure 3e was by far the best explanation of his data as presented (which contained several misrepresentations of characters), since it minimized Prendini's (2000) *ad hoc* modeling of scorpionoid neobothriotaxy, involving three characters which exhibited significantly high homoplasy. This problem was first noted by Soleglad & Sissom (2001: 71–72), further discussed by Soleglad & Fet (2003: 115–117), and finally resolved by Soleglad *et al*. (2005), and then again, by Fet & Soleglad (2006). In conclusion, one cannot necessarily predict the impact of implied weighting based only on the homoplasy index. Clearly, the severity of homoplasy on a character-by-character basis, as well as the position of these homoplasious characters on the tree, must also be considered. But clearly, in general, more homoplasious results will be affected more by this algorithm than the less homoplasious.

We were somewhat surprised that Francke & Prendini (2008) did not exercise bootstrap (and/or jackknife) sequences to demonstrate support for their impressive result. After all, Prendini (2000: fig. 2) applied bootstrap analysis to his scorpionoid result, generating not less than 10,000 pseudoreplicates. Since this particular analysis was not conducted by Francke & Prendini (2008) (or more correctly, was not presented in their paper), we exercised both bootstrap and jackknife sequences against their original data matrix (see Kitching, 1998, for a discussion on these two algorithms). We were further surprised to see that neither of these algorithms supported their result. Only a basal separation of subfamily Caraboctoninae (i.e., genera *Caraboctonus* and *Hadruroides*) from Hadrurinae (i.e., genera *Hadrurus* and *Hoffmannihadrurus*) was derived (Fig. 1). These sequences were exercised five times, 1000 pseudoreplicates per algorithm, a total of 10,000 pseudoreplicates. The cladogram shown in Fig. 1 is based on a majority-rule of the 10,000 pseudoreplicates, thus indicating that more than 50 % of these trees did not support the topology present in their figure 4. In order to further quantify this, we tabulated bootstrap/jackknife support values for the two clades of interest, "*gertschi* + *pinteri*", the crux of Francke & Prendini's result,

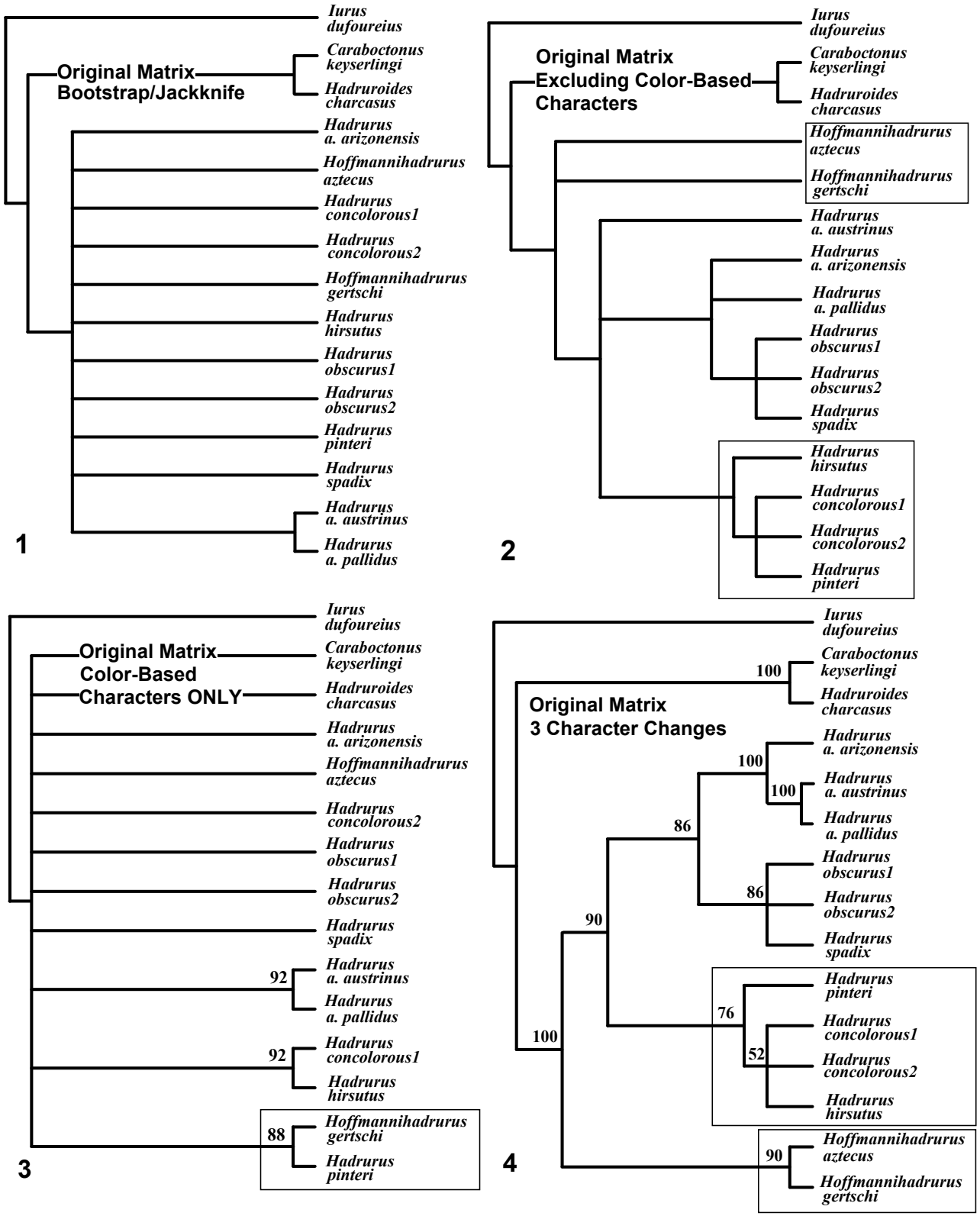

Fig. 1–4: Analysis of Francke & Prendini's (2008) cladistic results. Numbers above clades are percentage of MPTs supporting that node. Clades/taxa inside rectangles denote groupings of interest. **1.** Bootstrap/jackknife analysis of original data matrix (i.e., *no* changes) showing topology based on five separate sequences per algorithm, 1000 replicates each. Note, topology shows 50 % or more pseudoreplicate support, consequently, *none* of the results of Francke & Prendini (2008) are supported (see Table I). **2.** Majority-rule consensus of four MPTs of original data matrix with all color-based characters (1–8) suppressed. Note that separation of *Hoffmannihadrurus* species from *Hadrurus* and the clustering of *Hadrurus pinteri* with *H. hirsutus* and *H. concolorous*. **3.** Majority-rule consensus of 3760 MPTs of original data matrix with only color-based characters (1–8) considered. Note, clade "*Hoffmannihadrurus gertschi* + *Hadrurus pinteri*" has 88 % support while clade "*Hoffmannihadrurus aztecus* + *Hoffmannihadrurus gertschi*" only has 5.4 % support (not shown in figure, data derived from PAUP statistics). **4.** Majority-rule consensus of 21 MPTs of original data matrix with three character changes: suppression of character 32, and alterations to characters 8 and 44. Refer to discussion of these characters in this paper. Support data for this sequence: steps/CI/RI/G-fit = 59/0.7288/0.7419/-27.45. Numbers above clades are percentage of 21 MPTs that support that node.

and "*aztecus* + *gertschi*", a clade they refuted. Table I shows that only 44 % of the pseudoreplicates supported the former clade, the primary result of Francke & Prendini's "robust" analysis and the reason for their taxonomic emendation.

The character set of Francke & Prendini (2008: Appendix 3) embraces no less than eight characters devoted to coloration and its patterns (characters 1–8). After close examination of these characters, we see that two are coded specifically for the support of clade "*gertschi* + *pinteri*" (see their data matrix, tab. 4), four other characters support this clade (but not exclusively), and the only color-based character supporting clade "*aztecus* + *gertschi*" is rendered symplesiomorphic by nuanced state assignments to the outgroups. Although we will reject most of this character interpretation later in this paper, we were interested in seeing just what impact these color-based characters had on Francke & Prendini's "robust" result. To determine this, we exercised two cladistic analyses (sequences) using Francke & Prendini's original data matrix. The first of our sequences suppressed the eight color-based characters (leaving 24 informative characters), while the second suppressed all other characters except for the color-based characters (leaving just eight informative color-based characters). The results are quite revealing: for the first sequence (Fig. 2), where color-based characters are suppressed, we obtain a topology almost identical to that suggested by Fet *et al*. (2001) and modified by Fet *et al*. (2004), a topology rejected by Francke & Prendini (2008). Although not all groups are defined, clearly components of the clade "*aztecus* + *gertschi*" (i.e., *Hoffmannihadrurus*) are separated from *Hadrurus*. From this simple sequence alone, it is clear that Francke & Prendini's (2008) obtained their result "*gertschi* + *pinteri*" primarily from color considerations. To further support this claim, we observe that in the second cladistic sequence (Fig. 3), where *only* the coloration and its patterns are considered, we obtain a minimally resolved tree but, of importance to this discussion, we see that the clade "*gertschi* + *pinteri*" is well supported by 88 % of the 3760 MPTs (Most Parsimonious Trees). We might add that the result "*aztecus* + *gertschi*" in the second sequence was only supported by 5.4 % of the trees (not shown in figure, data derived from PAUP statistics).

Analysis of characters. Although we do not agree with much of Francke & Prendini's (2008) interpretation of characters and their suggested homologies, here we only identify the characters presented by these authors that, in our opinion, are incorrect not only in their interpretation, but are incorrect based on factual data as obtained from specimen examination. We identify three such characters:

Character-8: Metasoma, ventral surface, carinae, infuscation: not infuscated (0); infuscated (1). In this character, Francke & Prendini (2008) are addressing the colored pattern exhibited on the ventral carinae of metasomal segments I–IV. Unique in subfamily Hadrurinae are the conspicuously pigmented ventral carinae as found in *Hoffmannihadrurus* (see Williams, 1970b: fig. 11, for an illustration of this pigmentation in *Hoffmannihadrurus gertschi*). Only these four carinae, the ventrolateral and ventromedian pairs, are pigmented in two *Hoffmannihadrurus* species. In genus *Hadrurus*, there is no pigmentation on any of the metasomal carinae, except for those cases where the entire metasomal segment is pigmented. Francke & Prendini (2008) correctly code this pigmented state for the two *Hoffmannihadrurus* species but also propose that this condition is found in two of their outgroup species, *Caraboctonus keyserlingi* and *Hadruroides charcasus*. In general, all metasomal carinae are pigmented in *Hadruroides*, not just the ventral carinae, but only where granulation occurs. For example, in *H. charcasus*, the ventromedian carinae, which are essentially obsolete, are not pigmented, but instead subtle pigmentation is only present surrounding the paired setae. A similar condition is also found in *Hadruroides maculatus*. We do not consider this pigmentation seen in *Hadruroides* to be homologous to that found in *Hoffmannihadrurus*, which only occurs on the ventral carinal area, whether it is granulated, smooth, or obsolete. However, we will, in the context of this discussion, accept this "homologous" assignment to *Hadruroides* as assumed by Francke & Prendini (2008). At the same time, in the case of *Caraboctonus*, we reject this "homology" entirely. Adult *Caraboctonus* are very dark, almost dark brown to black in color. The dorsal carinal, where granulated, appear slightly darker than the intercarinal areas, again caused by specific granulation.

Consequently, in the original data matrix of Francke & Prendini (2008) we change the state of *C. keyserlingi* to "0" (i.e., ventral carinae not pigmented), while other character state settings remain unaltered.

Character-32: Pedipalp chela manus, external surface, accessory trichobothria in *Esb–Est* series: absent (0); present (1). Francke & Prendini (2008) modeled chelal external accessory trichobothria with two characters, 32 and 35. They decided to differentiate distal external accessory trichobothria on the palm from those found on the ventral edge of the palm, next to the ventroexternal carina (*V1*). For character 32, Francke & Prendini (2008) only attributed *Hadrurus pinteri* and *Hoffmannihadrurus gertschi* with accessory trichobothria whereas in character 35 they attributed this state not only to two aforementioned species but also to *Hadrurus hirsutus* and *H. concolorous*. We reject this dichotomy for two reasons: first, *H. hirsutus* and *H. concolorous* do exhibit accessory trichobothria on both areas of the palm, a fact which is even illustrated in Soleglad (1976: fig. 26). *Hadrurus hirsutus* exhibits minimal accessory trichobothria on the palm ventral edge, but in *H. concolorous* occurrence of accessory trichobothria in this area is quite prevalent, endorsing the accessory trichobothria loss hypothesis discussed further in this paper. Second, by creating two characters, Francke & Prendini's "*gertschi* + *pinteri*" clade is artificially bolstered as both characters support this (and only this) clade.

Since all four species exhibit external accessory trichobothria in both areas of the chelal palm, making this alteration to character 32 renders it identical to character 35. Therefore, we eliminate character 32, ending up with character 35 attributing external accessory trichobothria to all four species (note that leaving both characters results in effectively assigning this condition a weight of 2).

Character-44: Pedipalp chela, trichobothrium *ib* position: on manus, behind movable finger condyle (0); basal on

Table I. Bootstrap/jackknife support for clades "*Hoffmannihadrurus gertschi* + *Hadrurus pinteri*" and "*Hoffmannihadrurus aztecus* + *Hoffmannihadrurus gertschi*". The table compares statistical support for the results of: original analysis conducted by Francke & Prendini (2008); Francke & Prendini (2008) original analysis with three changes*; the latter but with three *new* characters added; and the three new analyses presented in this paper. Each bootstrap and jackknife sequence (five separate sequences per support type) produced 1000 pseudoreplicates, 5000 per support type, a total of 10000 per result. The data are presented as minimum–maximum (mean) values. See Fig. 26 for a more expanded bootstrap/jackknife data for the new analysis involving all characters. *Modified data matrix involved three changes as discussed in this paper.

		"*gertschi* + *pinteri*"	"*aztecus* + *gertschi*"
Francke & Prendini (2008) Original Analysis	Bootstrap	**42.2–46.7 (44.08) %**	21.0–24.4 (22.66) %
	Jackknife	**43.0–45.7 (44.38) %**	21.1–22.5 (21.96) %
Francke & Prendini (2008) Original Analysis Modified*	Bootstrap	30.5–31.7 (31.10) %	**52.8–54.7 (53.70) %**
	Jackknife	31.4–34.3 (33.64) %	**45.3–48.9 (47.18) %**
Francke & Prendini (2008) Original Analysis Modified* Plus three *new* characters	Bootstrap	8.5–12.7 (10.72) %	**70.5–73.4 (72.12)** %
	Jackknife	10.4–11.1 (10.74) %	**66.6–68.1 (67.40)** %
New Analysis Fundamental Characters	Bootstrap	Under 5 %	**67.2–67.8 (67.58) %**
	Jackknife	Under 5 %	**66.1–66.8 (66.48) %**
New Analysis Low-level Characters	Bootstrap	Under 5 %	**68.4–70.0 (69.24) %**
	Jackknife	Under 5 %	**72.6–73.2 (72.86) %**
New Analysis All characters	Bootstrap	Under 5 %	**98.4–98.8 (98.58) %**
	Jackknife	Under 5 %	**96.3–97.0 (96.60) %**

fixed finger (1); suprabasal on fixed finger (2). This character and its state settings are by far the most obvious misrepresentation of observable data. Francke & Prendini (2008) used the terminology of Fet *et al*. (2004), "basal" and "suprabasal", to render a clearly derived character for clade "*aztecus* + *gertschi*" symplesiomorphic by assigning the position of trichobothrium *ib* the same state setting as in the outgroup taxa *Caraboctonus* and *Hadruroides*. In Fet *et al*. (2004: key on p. 23), the terms "basal" and "suprabasal" were used to relatively distinguish *Hadrurus* from *Hoffmannihadrurus*. When Francke & Prendini (2008) included *Iurus dufoureius* in their outgroup set, they distinguished the *ib* position as "behind movable finger condyle" in *Iurus*, "basal" in *Caraboctonus*, *Hadruroides*, *Hoffmannihadrurus*, and "suprabasal" in *Hadrurus*. It is clear in our Figure 5 that four relative *ib* positions are observed, not three: (1) on the palm, well proximal of movable finger juncture (*Chaerilus*, *Calchas*, and *Iurus*); (2) adjacent to movable finger juncture at the distal aspect of articulation membrane (*Caraboctonus* and *Hadruroides*); (3) basal on fixed finger (*Hoffmannihadrurus*); and (4) suprabasal on fixed finger (*Hadrurus*). We might add here that we verified the position of trichobothria *ib*–*it* in *Caraboctonus* and *Hadruroides* (involving two species) on both chelae, involving all 17 specimens available to us. Since Francke & Prendini (2008: Appendix 2) examined no less than 21 specimens of *Caraboctonus keyserlingi* and 16 specimens of *Hadruroides charcasus*, we are surprised at their misinterpretation of this character and its state mappings for these taxa.

Consequently, in the original data matrix we change character 44 to include four state values: "0" for *Iurus*, "1" for *Caraboctonus* and *Hadruroides*, "2" for *Hadrurus* species, and "3" for *Hoffmannihadrurus* species.

Result: The changes described above to three characters in the original data matrix of Francke & Prendini (2008) resulted in a cladistic analysis yielding a topology identical to that presented in Fet *et al*. (2001: fig. 15) as modified by Fet *et al*. (2004), a result *rejected* by Francke & Prendini (2008). In Fig. 4, we show the consensus of 21 MPTs where *Hoffmannihadrurus* and *Hadrurus* monophyly is supported by 90 % of the trees. In addition, in Table I, we show that bootstrap analysis supports this result (but not Francke & Prendini's (2008) original analysis), with jackknife showing 47 %, not quite a consensus. It must be stressed here that this totally different result was based on Francke & Prendini's (2008) original data matrix with the alteration of *only three characters*— a result where the clade "*aztecus* + *gertschi*" exhibited higher bootstrap/jackknife support than Francke & Prendini's original result of clade "*gertschi* + *pinteri*", roughly a 22 % / 6 % improvement per algorithm. Note that, if we augment Francke & Prendini's (2008) modified result with *three new characters* discussed in our cladistic analysis that further support the monophyly of *Hoffmannihadrurus* (see characters 27–29 below)—all of which are irrefutable characters, presumably unknown to Francke & Prendini (2008)—we again obtain the topology in Fig. 4 with a 72/67 bootstrap/jackknife support for clade "*aztecus* + *gertschi*" (and 11/11 support for clade "*gertschi* + *pinteri*", see Table I).

Final observations that we are compelled to make, are:

(1) based on a detailed examination of our material and a careful survey of past literature, we isolated no less than four new characters that support the monophyly of genus *Hoffmannihadrurus*, three of which were even discussed by other authors. We find it strange that Francke & Prendini (2008) did not uncover one or more of these characters during their exhaustive examination of 170 *Hadrurus* and *Hoffmannihadrurus* specimens;

(2) Francke & Prendini (2008) write: "…According to the optimal tree retrieved in the present analyses (Fig. 4), the absence of internal accessory trichobothria on the pedipalp chela fixed finger is plesiomorphic in *H. aztecus* and undergoes an autapomorphic reversal (interpreted as loss of the trichobothria) in *H. gertschi*, falsifying this character state as a diagnostic synapomorphy of *Hoffmannihadrurus.*" We find it unfortunate that these authors would so casually suggest such a reversal in trichobothrial evolution. Trichobothrial patterns are one of the most important, complex, and well studied character sets in scorpion systematics (Vachon, 1974; Soleglad & Fet, 2001), and their changes and homologies have to be addressed seriously. This attitude to trichobothrial information is even more remarkable when one realizes that Francke & Prendini's phylogeny, the reason for this statement, was based primarily on *coloration and its patterns*, which is a truly low-level and localized character set.

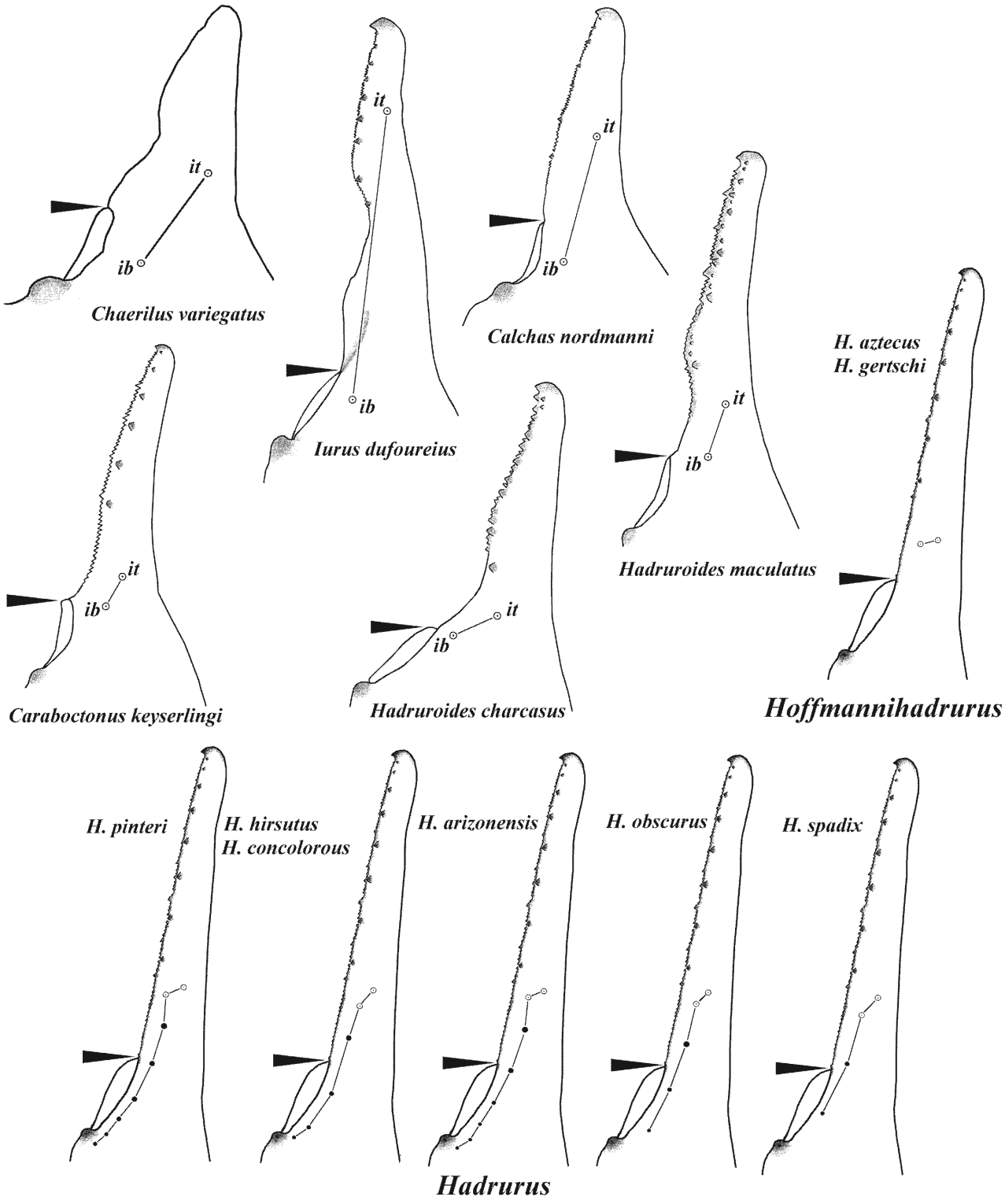

Fig. 5. Position of trichobothrial series *ib–it* in superfamily Iuroidea and outgroup *Chaerilus*. Illustrations show internal view of chelal fixed finger including internal condyle and articulation membrane. Trichobothria *ib–it* are represented with open circles, internal accessory (*ia*) trichobothria in *Hadrurus* are represented by solid circles, the smaller sizes depicting their petite nature in the more basal areas. Black arrow indicates internal juncture of movable finger at membrane. Relative locations of trichobothrium *ib* are based on this juncture: in *Chaerilus*, *Iurus*, and *Calchas*, *ib* is located on the chelal palm, proximal of this juncture; in *Caraboctonus* and *Hadruroides*, *ib* is located adjacent to this juncture; in *Hoffmannihadrurus* and *Hadrurus*, *ib* is located on the fixed finger distal of this juncture, basally situated in *Hoffmannihadrurus* and suprabasally in *Hadrurus*.

Cladistic Analysis of Iuroidea

In this section we present our own cladistic analysis of superfamily Iuroidea based on detailed analysis of all material representing our outgroup and ingroup taxa. This analysis serves as the basis for reinstating genus *Hoffmannihadrurus*, rejected by Francke & Prendini (2008).

In our cladistic treatment, we conduct three separate analyses (sequences) in a "layered" fashion, each one successively adding new characters to the previous sequence:

1) fundamental characters: "high-level" characters, presumably derived earlier in (at higher levels of) scorpion evolution (characters 1–29)

2) low-level characters: characters specific to subfamily Hadrurinae, involving coloration and its patterns, setation, and the telson aculear gland (characters 30–37)

3) characters relating to our accessory trichobothria loss hypothesis: three characters that model the reduction of neobothriotaxy in subfamily Hadrurinae (characters 38–40)

The purpose of this stepwise, "layered" approach to cladistic analysis is to get a better understanding of character evolution and to demonstrate basic topologies with the *minimal set of assumptions*. As will be shown below, the overall genus-level topology, which supports the six genera of Iuroidea, is achieved with a set of characters that do not involve any hypotheses of character evolution. This result alone supports the monophyly of our genus *Hoffmannihadrurus*. The second two analyses deal with characters primarily specific to subfamily Hadrurinae. In general, we do not believe that localized, phenotypically variable characters such as coloration and its patterns, or setation, are relevant at higher levels of analysis; to "map their polarity" by progressing upwards into the outgroups, in our opinion, is essentially nonsensical. Most polarities of this nature are only determinable from the immediate common ancestor of two clades, thus coding similar data for higher levels is meaningless and therefore we consider it "inapplicable". We acknowledge that this decision is context-dependent and in itself is an assumption.

Outgroup and ingroup selection

Soleglad & Fet (2003b: fig. 114, 110) suggested that Iuroidea was the most plesiomorphic superfamily in parvorder Iurida, a hypothesis we support here. Based on the analysis of Soleglad & Fet (2001, 2003b) and Baptista *et al*. (2006), who demonstrated that Chaerilida is the sister parvorder to Iurida, we choose *Chaerilus variegatus* to be our outgroup. *Chaerilus*, the only extant genus of Chaerilida, proves to be an excellent outgroup since we see several presumed shared characters between Chaerilida and Iuroidea: Trichobothria *ib–it* alignment on the fixed finger; oblique and imbricating chelal median denticle (*MD*) rows; 8-carinae configuration of the chela; a single subdistal (*sd*) denticle on the cheliceral fixed finger dorsal edge; genital papillae arrangement in the male, all shared in Iuroidea, in particular family Iuridae, thus proposed as symplesiomorphic. The family Caraboctonidae, which demonstrates significant derivations from its sister family Iuridae, inherits only the oblique *MD* denticle groups.

Our ingroup selection includes members of all six genera comprising Iuroidea: *Calchas*, *Iurus*, *Caraboctonus*, *Hadruroides* (two species out of nine), *Hoffmannihadrurus* (two species), and *Hadrurus* (six species). Except for the genus *Hadruroides*, all species in this superfamily are included. At a species level, the primary goal of this analysis pertains to subfamily Hadrurinae and its two genera, thus the exclusion of some *Hadruroides* species is inconsequential. In presenting subspecies of *Hadrurus*, we follow results of Fet *et al*. (2001) molecular (mtDNA) analysis that demonstrated that *H. arizonensis pallidus* Williams, 1970 is synonymous with the nominotypical subspecies *H. arizonensis arizonensis*. It is interesting to mention that observations of *Hadrurus arizonensis* in laboratory (S. Tallarovic, pers. comm.) recorded dark and pale phenotypes from the same population, indeed born from the same female. Note that Francke & Prendini (2008) consider *H. a. pallidus* a valid subspecies (based on coloration characters alone), although they *did not* formally declare that *H. a. pallidus* is returned from synonymy with *H. a. arizonensis*. Therefore we do not have to declare a new synonymy here since *H. a. pallidus* was never formally reestablished. Since the subspecies *H. arizonensis austrinus* was not available for the DNA study of Fet *et al*. (2001), we include it in our taxa set. The inclusion of "dark" and "pale" forms of *H. concolorous* and *H. obscurus* as separate taxa, as suggested in Francke & Prendini's (2008) study, in our opinion, is not warranted, and is not considered in this study. Furthermore, for the latter species, Fet *et al*. (2001: table 1) showed that the dark and pale forms of *H. obscurus* exhibited zero DNA difference, as similarly observed for *H. a. arizonensis* and *H. a. pallidus*.

Cladistic characters

All 40 characters are described below, partitioned into the three categories outlined above. The results of each successive cladistic analysis follow each character set.

Character specifics: We now describe the assumptions, support characteristics, and distribution data of each character, grouped and ordered by its character type within the three character partitions described above. For each character we describe the following: character number and description, its state values and descriptions, its characteristics (assumptions | tree steps | CI (consistency index) | RI (retention index) | G-Fit (Goloboff Fit)), and its distribution across clades as illustrated in Fig. 26. [default GOLOBOFF mode value is set to 2, from a 0–5 range; see Kitching *et al*., 1998, and Goloboff, 1993, for more information and definitions of these terms].

Assumptions imply an *ordering*, which we categorize into three types: 1) a primary character and one or more secondary, tertiary, etc. characters; 2) fully ordered character states; and 3) partially ordered character states using PAUP's USERTREE schematic definition feature. The first ordering technique, which uses two or more characters, forces ordering by assigning a presumed primitive state to a set of taxa, and then defining one or more derivations from this state with additional characters. This ordering approach is also known as an "additive" technique commonly used in "single-state" character definition schemes. Straight ordering allows a linear ordering between three or more states, and partial ordering allows the definition of complex "or-

dered trees". None of these ordering mechanisms forces polarity, which is determined by the parsimony process.

Each character and its distribution by state are shown in Figure 26, which represents the complete cladistic result based on morphology (characters 1–40). Character number is found above the rectangle, its state value is found below. If the character is homoplasious, the rectangle is open (white), otherwise it is black. The letters of "U", "A", and "D" mean the following: "U" = unambiguous distribution; "A" = distribution based on accelerated optimization (ACCTRAN in PAUP); and "D" = distribution based on delayed optimization (DELTRAN in PAUP). If the character is not marked with a letter, it distributes consistently for both "A" and "D" sequences. Also, character/state pairs marked with an "A" are always matched with an accompanying character/state marked with a "D". The "A" character is always situated higher (i.e., closer to the root) in the cladogram. See Table III for the data matrix showing the state assignments of these characters to the taxa.

Out of the 40 characters addressed in this analysis, seven characters are uninformative (noted below). Note that these seven characters are included in our discussion which follows and are shown distributed on the cladogram in Figure 26. By convention, state value "one" of an uninformative character is shown in the cladogram (Fig. 26). The retention index (RI) is undefined for uninformative characters because the minimal number of steps is equal to the maximum number, and therefore is indicated with a "-" in the characteristics statements below. The seven uninformative characters are suppressed in the calculations of tree support.

For most characters, one or more references are provided for additional information. In the cases where new analysis is presented, the character is discussed further.

In all bootstrap and jackknife analyses, five sequences were initiated and the mean value is reported in our text and Figures. For most comparative analyses, five sequences of 1000 pseudoreplicates per algorithm were initiated, but in the final cladogram (Fig. 26), five sequences of 10,000 pseudoreplicates per algorithm are shown.

(1) Fundamental Characters

Character 1: Sternum type (**0:** type 1; **1:** type 2); characteristics = (none | 1 | 1.000 | - | 1.000). This character is *uninformative*, outgroup *Chaerilus* exhibiting a type 1 sternum, the ingroup with a type 2 sternum. This character is unambiguously distributed for the superfamily Iuroidea, which has a type 2 sternum. See Soleglad & Fet (2003a) for information on this character.

Character 2: Orthobothriotaxic type (**0:** type B; **1:** type C); characteristics = (none | 1 | 1.000 | - | 1.000). This character is *uninformative*, outgroup *Chaerilus* complying with type B orthobothriotaxy and the ingroup with type C. This character is unambiguously distributed for the superfamily Iuroidea, which has type C orthobothriotaxy. See Vachon (1974) for information on this character.

Character 3: Hemispermatophore type (**0:** fusiform type; **1:** lamelliform type); characteristics = (none | 1 | 1.000 | - | 1.000). This character is *uninformative*, outgroup *Chaerilus* having a fusiform hemispermatophore and the ingroup with lamelliform type. This character is unambiguously distributed for the superfamily Iuroidea, which has lamelliform type. See Stockwell (1989) for information on this character.

Character 4: Leg tarsus spination/setation type (**0:** type 2A; **1:** type 3); characteristics = (none | 1 | 1.000 | - | 1.000). This character is *uninformative*, outgroup *Chaerilus* conforming to type 2A and the ingroup with type 3 (i.e., medially ordered row of spinule clusters). This character is unambiguously distributed for the superfamily Iuroidea, which has type 3. See Soleglad & Fet (2003b: 17–19) and Fet *et al*. (2004) for information on this character.

Character 5: Chelal finger median denticle (*MD*) row arrangement (**0:** oblique and imbricating; **1:** oblique and non-imbricating); characteristics = (none | 1 | 1.000 | 1.000 | 1.000). This character is unambiguously distributed for the family Caraboctonidae, which has *MD* rows oblique but not imbricating. The outgroup *Chaerilus* and family Iuridae have oblique imbricating *MD* rows. See Soleglad & Sissom (2001: 40) for information on this character.

Character 6: Chelal carinae configuration (**0:** 8-carinae configuration; **1:** 10-carinae configuration); characteristics = (none | 1 | 1.000 | 1.000 | 1.000). This character is unambiguously distributed for the family Caraboctonidae, which has pedipalp chelae with the 10-carinae configuration. The outgroup *Chaerilus* and family Iuridae conform to the 8-carinae configuration. See Soleglad & Sissom (2001: 41–42) for information on this character.

Character 7: Number of cheliceral fixed finger subdistal (*sd*) denticles (**0:** one *sd*; **1:** two *sd*); characteristics = (none | 1 | 1.000 | 1.000 | 1.000). This character is unambiguously distributed for the family Caraboctonidae, which has cheliceral movable finger with two *sd* denticles. The outgroup *Chaerilus* and family Iuridae exhibit a single *sd* denticle. See Vachon (1963) and Soleglad & Fet (2003b) for information on this character.

Character 8: Ventral accessory (*va*) denticles found on cheliceral fixed finger (**0:** *va* denticles present; **1:** *va* denticles absent); characteristics = (none | 1 | 1.000 | - | 1.000). This character is *uninformative*, outgroup *Chaerilus* exhibiting conspicuous *va* denticles and the ingroup without these denticles. This character is unambiguously distributed for superfamily Iuroidea, which has cheliceral fixed finger without *va* denticles. See Soleglad & Fet (2003b) for information on this character.

Character 9: Ventral accessory (*va*) denticles found on cheliceral movable finger (**0:** with many small *va* denticles; **1:** with one large conspicuous *va* denticle); characteristics = (none | 1 | 1.000 | - | 1.000). This character is *uninformative*, outgroup *Chaerilus* exhibiting many small *va* denticles and the ingroup with one large *va* denticle. This character is unambiguously distributed for superfamily Iuroidea, which has cheliceral movable finger with one large *va* denticle. See Soleglad & Fet (2003b) for information on this character.

Character 10: Genital papillae in male (**0:** without posterior extensions, visible between sclerites; **1:** posterior extensions present, visible below posterior edge of sclerites; **2:** absent); characteristics = (none | 2 | 1.000 | 1.000 | 1.000). The outgroup *Chaerilus* and family Iuridae lack posterior extensions, the papillae only visible between the sclerites. The presence of posterior extensions (state = 1) distribution

differs in optimization sequences, it either distributes for family Caraboctonidae if accelerated or subfamily Caraboctoninae if delayed. The absence of genital papillae (state = 2) distributes consistently for subfamily Hadrurinae.

Character 11: Position of chelal trichobothrium *ib* (**0:** on palm, proximal of movable finger inner juncture; **1:** adjacent to movable finger inner juncture; **2:** basal on fixed finger, distal of movable finger inner juncture; **3:** suprabasal on fixed finger, distal of movable finger inner juncture); characteristics = (none | 3 | 1.000 | 1.000 | 1.000). Location of *ib* adjacent to movable finger juncture (state = 1) is distributed for family Caraboctonidae if optimization is accelerated, otherwise for subfamily Caraboctoninae if delayed. Location of *ib* basal on fixed finger (state = 2) is distributed for subfamily Hadrurinae if accelerated and for genus *Hoffmannihadrurus* if delayed. Suprabasal position of *ib* on fixed finger (state = 3) is consistently distributed for genus *Hadrurus*.

Figure 5 illustrates trichobothrium *ib* position on all species considered in this analysis. As emphasized elsewhere in this paper, Francke & Prendini (2008), in our opinion, incorrectly interpreted this character for subfamily Caraboctoninae (i.e., genera *Caraboctonus* and *Hadruroides*). It is clear from Fig. 5 that the position of *ib* in Caraboctoninae is *not* the same as (i.e. not homologous) to that exhibited in genus *Hoffmannihadrurus*. We examined both chelae from three caraboctonine species (a total of 34 pedipalps), and in all cases *ib* was located at the extreme base of the fixed finger adjacent to the inner juncture of the movable finger. It is also interesting to note that the overall alignment of the *ib–it* series in Caraboctoninae is similar to that seen in Iuridae (and *Chaerilus* for that matter), but the spacing between the two trichobothria is much smaller, *it* not as far placed on the fixed finger. In subfamily Hadrurinae, *ib–it* alignment differs from that seen in Caraboctoninae, the two trichobothria in hadrurines being much closer to each other.

Character 12: Relative distance between trichobothria *ib* and *it* (**0:** distance large, *it* located at least at finger midpoint; **1:** distance relatively small, *it* always well proximal of finger midpoint); characteristics = (none | 1 | 1.000 | 1.000 | 1.000). This character is unambiguously distributed for the family Caraboctonidae, where distance between *ib–it* is relatively small. For outgroup *Chaerilus* and family Iuridae, the distance is large. See Figure 5.

Character 13: Presence of *additional* petite trichobothria on chela (type C only): *Est*, esb_2, and V_2 (**0:** three additional petite trichobothria present; **1:** not present; **-:** not applicable); characteristics = (none | 2 | 1.000 | 1.000 | 1.000). This character is inapplicable for the outgroup *Chaerilus* because it only pertains to type C orthobothriotaxy. The absence of these additional petite trichobothria is consistently distributed for family Caraboctonidae, which has fully developed trichobothria; they are petite in Iuridae. See Vachon (1974: figs. 212–213, 216–217) for information on this character.

Character 14: Presence of *additional* petite trichobothria on patella external surface (type C only): eb_2, et_2 (**0:** two additional petite trichobothria present; **1:** not present; **-:** not applicable); characteristics = (none | 2 | 1.000 | 1.000 | 1.000). This character is inapplicable for the outgroup *Chaerilus* because it only pertains to type C orthobothriotaxy. The absence of these additional petite trichobothria is distributed consistently for family Caraboctonidae, which has fully developed trichobothria; they are petite in Iuridae. See Vachon (1974: figs. 214, 218) for information on this character.

Character 15: Patellar trichobothrium v_2 location (type C only) (**0:** external surface; **1:** ventral surface; **-:** inapplicable); characteristics = (none | 2 | 1.000 | 1.000 | 1.000). This character is inapplicable for the outgroup *Chaerilus* because it only pertains to type C orthobothriotaxy. The ventral location of v_2 is distributed consistently for family Caraboctonidae, but in Iuridae v_2 is located externally. See Vachon (1974: figs. 214, 218) for information on this character.

Character 16: Position of chelal trichobothrium Et_5 (type C only) (**0:** grouped with Et_4, on palm; **1:** removed from Et_4, on fixed finger; **-:** inapplicable); characteristics = (none | 2 | 1.000 | 1.000 | 1.000). This character is inapplicable for the outgroup *Chaerilus* because it only pertains to type C orthobothriotaxy. The fixed finger location of Et_5 is distributed consistently for family Caraboctonidae; it is located on the palm in Iuridae. Note that this character homology for subfamily Caraboctoninae is based upon Stockwell's (1989: figs. 175–176) interpretation. See Soleglad & Fet (2003b: fig. 65) for more information on this character.

Character 17: Neobothriotaxy of pedipalp (type C only) (**0:** not present; **1:** minor neobothriotaxy on patella external surface; **2:** major neobothriotaxy on chela and patella; **-:** inapplicable); characteristics = (see below | 3 | 1.000 | 1.000 | 1.000). This character is inapplicable for the outgroup *Chaerilus* because it only pertains to type C orthobothriotaxy. The family Iuridae lacks neobothriotaxy (state = 0). The minor neobothriotaxy (state = 1) distribution differs in optimization sequences; it either appears in family Caraboctonidae if accelerated or in subfamily Caraboctoninae if delayed. The presence of major neobothriotaxy (state = 2) is distributed consistently for subfamily Hadrurinae.

This character (state = 2) can be interpreted in two ways: 1) for the fundamental character cladistic analysis (characters 1–29), it only requires that major neobothriotaxy is present in Hadrurinae, in contrast to the minor neobothriotaxy (i.e., a single accessory trichobothrium) seen in Caraboctoninae; 2) for the further breakdown of species groups in Hadrurinae (see characters 38–40), the character assumes (part of a hypothesis) that the common ancestor of genera *Hoffmannihadrurus* and *Hadrurus* exhibited major neobothriotaxy in all areas of the chela (internal, external, and ventral surfaces) and the patella (external and ventral surfaces). This assumption is the first and necessary part of the accessory trichobothria loss hypothesis; the second part (see discussions for characters 38–40 below) assumes successive losses of these accessory trichobothria during various levels of speciation and further evolution within Hadrurinae. It is important to note here that the cladistic analysis based on fundamental characters (see Fig. 22) neither requires nor assumes this hypothesis, thus exercising the first interpretation of this character.

Character 18: Position of trichobothria *Db* and *Dt* (type C only) (**0:** *Db* basal on palm, *Dt* distal; **1:** *Db* and *Dt* distal on palm; **2:** *Db* and *Dt* basal on palm; **-:** inapplicable); charac-

teristics = (none | 3 | 1.000 | 1.000 | 1.000). This character is inapplicable for the outgroup *Chaerilus* because it only pertains to type C orthobothriotaxy. The family Iuridae has *Db* and *Dt* disjoint on the palm (state = 0). The distal placement of both *Db* and *Dt* (state = 1) distribution differs in optimization sequences, it either appears in family Caraboctonidae if accelerated or for subfamily Caraboctoninae if delayed. The basal placement of both *Db* and *Dt* (state = 2) is consistently distributed for subfamily Hadrurinae. Note that this character homology for subfamily Caraboctoninae is based upon Stockwell's (1989: figs. 175–176) interpretation. See Soleglad & Fet (2003b: fig. 65) for more information on this character.

Character 19: Leg unguicular spine (**0:** well developed, pointed; **1:** blunted, not pointed); characteristics = (none | 1 | 1.000 | 1.000 | 1.000). This character is unambiguously distributed for the subfamily Caraboctoninae, where the unguicular spine is blunted. See Fet *et al*. (2004: figs. 9, 14) for information on this character.

Character 20: Spinule cluster configuration on leg tarsus (type 3 only) (**0:** irregular placed spinule clusters on juveniles, found basally on adults; **1:** well-formed spinule cluster clumps; **2:** fused-clusters, well defined; **3:** fused-clusters, weakly defined; **-:** inapplicable); characteristics = (none | 3 | 1.000 | 1.000 | 1.000). This character is inapplicable for the outgroup *Chaerilus* because it only pertains to leg tarsus spination type 3. Spinule cluster clumps (state = 1) are considered primitive for superfamily Iuroidea. Irregular placed spinule clusters (state = 0) is unambiguously distributed for genus *Calchas*. The well defined fused-clusters (state = 2) distribution differs in optimization sequences; it either appears in subfamily Hadrurinae if accelerated or for genus *Hadrurus* if delayed. The weakly defined fused-clusters (state = 3) is consistently distributed for genus *Hoffmannihadrurus*. See Fet *et al*. (2004) for more information on this character.

Character 21: Tibial spurs on legs III and IV (**0:** tibial spurs absent; **1:** tibial spurs present); characteristics = (none | 1 | 1.000 | - | 1.000). This character is *uninformative*; only genus *Calchas* in our taxa set exhibits tibial spurs, where it is distributed unambiguously. See Vachon (1971: fig. 12) for information on this character.

Character 22: Leg pedal spurs (**0:** smooth; **1:** with spinelets); characteristics = (none | 1 | 1.000 | 1.000 | 1.000). Pedal spurs with spinelets are distributed unambiguously for subfamily Hadrurinae.

Character 23: Carapace anterior edge (**0:** essentially straight; **1:** subtle to deep indentation; **2:** highly convexed); characteristics = (none | 2 | 1.000 | 1.000 | 1.000). Carapaces with an anterior indentation are distributed consistently for family Iuridae, and highly convexed carapaces are distributed consistently for family Caraboctonidae. See Fet *et al*. (2004: figs. 53–58) for more information on this character.

Character 24: Carapace ocular carinae (**0:** weak to obsolete; **1:** well defined); characteristics = (none | 1 | 1.000 | 1.000 | 1.000). Well defined ocular carinae are unambiguously distributed for family Iuridae. See Fet *et al*. (2004: figs. 53–58) for more information on this character.

Character 25: Chelal finger inner accessory (*IAD*) and outer accessory (*OAD*) denticles (**0:** absent; **1:** present); characteristics = (none | 1 | 1.000 | 1.000 | 1.000). The presence of *IAD* and *OAD* denticles is unambiguously distributed for genus *Hadruroides*. See Soleglad & Sissom (2001: fig. 34) for more information on this character.

Character 26: Number of inner (*ID)* denticles on chelal movable finger (**0:** variable; **1:** fixed number, seven; **2:** fixed number, nine; **3:** fixed number, 15); characteristics = (none | 3 | 1.000 | 1.000 | 1.000). Seven *ID* denticles condition (state = 1) is distributed consistently for superfamily Iuroidea. Fifteen *ID* denticles condition (state = 3) is distributed unambiguously for genus *Iurus* and nine *ID* denticles condition (state = 2) is distributed unambiguously for subfamily Hadrurinae.

Character 27: Pedipalp dorsal and ventral patellar spur (*DPS*, *VPS*) development (**0:** area concaved, *DPS*/*VPS* absent; **1:** *DPS*/*VPS* present, spurs doubled; **2:** *DPS*/*VPS* present, spurs single; **3:** *DPS*/*VPS* obsolete, proximal area flat; **4:** *DPS*/*VPS* obsolete, proximal area with conspicuous projection); characteristics = (none | 4 | 1.000 | 1.000 | 1.000). The occurrence of doubled *DPS*/*VPS* (state = 1) distribution is dependent on the optimization sequence, distributed for superfamily Iuroidea if accelerated and family Iuridae if delayed. Similarly, for *DPS*/*VPS* with single spurs (state = 2), it is distributed for family Caraboctonidae if accelerated and subfamily Caraboctoninae if delayed. Absence of the *DPS*/*VPS* structures with a flat proximal area (state = 3) distributes for subfamily Hadrurinae if accelerated and distributes for genus *Hadrurus* if delayed. Absence of the *DPS*/*VPS* structures with a prominent projection on the proximal area (state = 4) distributes consistently for genus *Hoffmannihadrurus*. See Soleglad & Sissom (2001: 59) for information concerning the *DPS*/*VPS* structures in *Iurus* and *Calchas*.

Figures 6–13 show the dorsal view of the pedipalp patella for all eight species comprising genera *Hoffmannihadrurus* and *Hadrurus*. As is readily clear in Figs. 6–7, *Hoffmannihadrurus gertschi* and *H. aztecus* have a conspicuous projection on the basal aspect of the internal surface of the patella. In *Hadrurus* species (Figs. 8–13), this area is quite flat, only exhibiting a small raised portion. To supplement these eight photographs we present a morphometric ratio in Table II based on measurements of this basal projection as it relates to the width of the patella at that position (see Table II for specifics on these measurements). As can be seen from the data in Table II, the height of the basal projection in *Hoffmannihadrurus* is roughly 24 % of the patella width whereas in *Hadrurus* the minimal projection is less than 10 % of the patella's width. The mean value difference between these two ratio values exceeds 160 %.

Character 28: Chelal palm development (carinae-10 configuration only) (**0:** palm rounded, carinae somewhat weak, but digital (*D1*) and external (*E*) carinae developed; **1:** palm vaulted dorsally, much deeper than wide, *D1* and *E* carinae essentially obsolete: dorsosecondary (*D3*) and dorsomarginal (*D4*) carinae rounded basally, covered with coarse granulation, intercarinal area narrow due to dense granulation; **2:** palm vaulted dorsally, much deeper than wide, *D1* and *E* carinae essentially obsolete: *D3* and *D4* carinae not rounded basally but discretely formed, not covered with coarse granulation, intercarinal area wide, distinct and smooth; **-:** inapplicable); characteristics = (none | 3 | 1.000 | 1.000 |

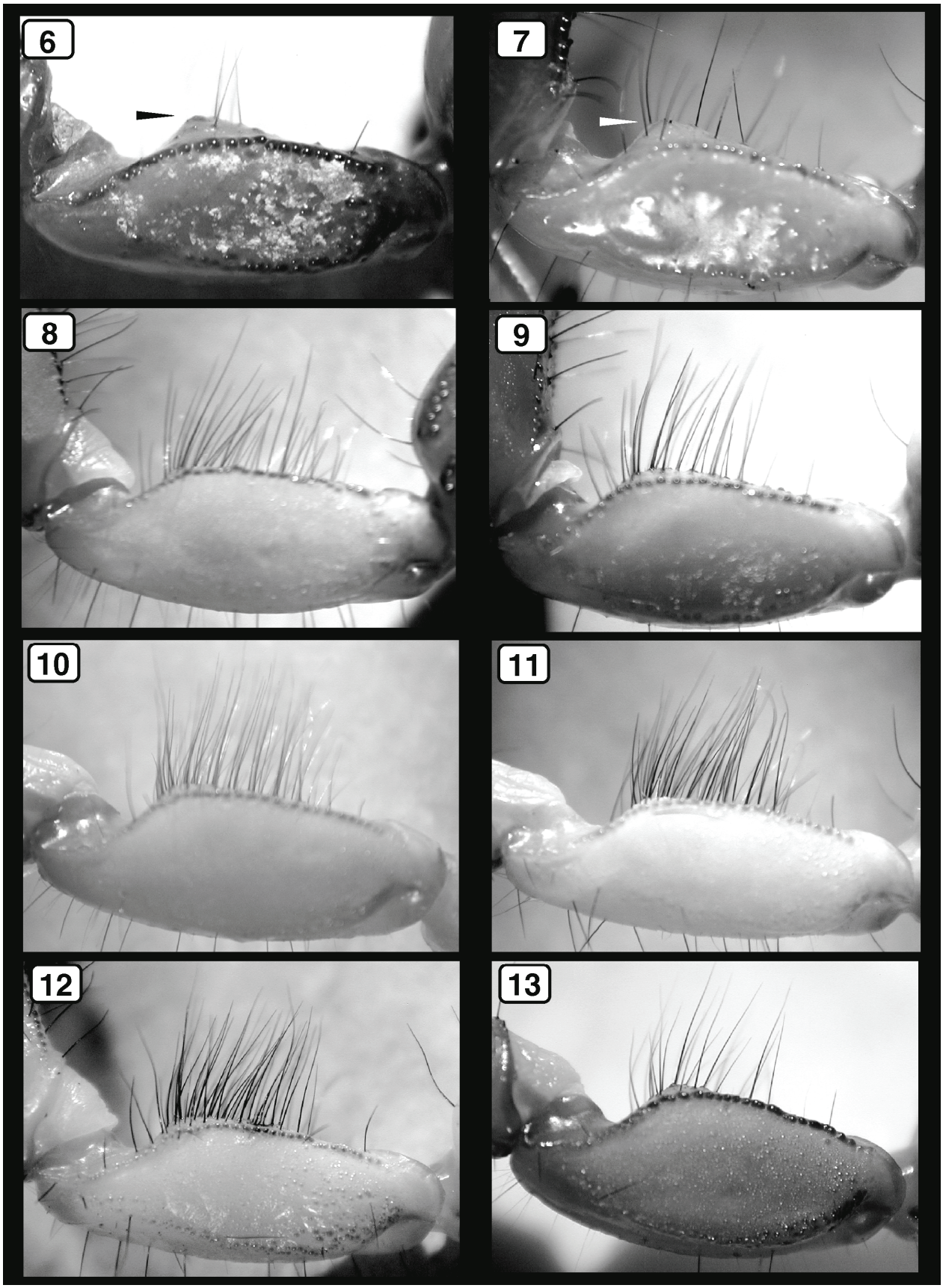

Fig. 6-13. Structure and setation of internal surface of pedipalp patella for genera *Hoffmannihadrurus* and *Hadrurus*. Arrow indicates conspicuous projection on basal aspect of patella in *Hoffmannihadrurus* which is absent in *Hadrurus*. See Table II for setation statistics. **6.** *Hoffmannihadrurus gertschi*, female, Iguala, Guererro, Mexico. Note many of the setae are broken off in this specimen, the actual setal number based on bristles and areolae is 14. **7.** *Hoffmannihadrurus aztecus*, male, Tehuacan, Puebla, Mexico. **8.** *Hadrurus pinteri*, male, Oakies Landing, Baja California, Mexico. **9.** *Hadrurus concolorous*, male, Santa Rosalia, Baja California Sur, Mexico. **10.** *Hadrurus arizonensis*, male, Carizzo Badlands, ABDSP, California, USA. **11.** *Hadrurus obscurus*, male, Pinyon Mountain, ABDSP, California, USA. **12.** *Hadrurus spadix*, male, Winnemucca, Humboldt Co., Nevada, USA. **13.** *Hadrurus hirsutus*, male, Cabo San Lucas, Baja California Sur, Mexico.

Table II. Statistical data on pedipalp patella for genera *Hoffmannihadrurus* and *Hadrurus*. Morphometric ratio of patellar internal basal projection *DI*|*DE* / projection height: *DI* = dorointernal carina; *DE* = dorsoexternal carina. *DI*|*DE* = distance between *DI* and *DE* anchored at center of projection base. Projection height = distance from *DI* to distal tip of projection.

	Morphometric Ratio of Patellar Internal Basal Projection (♂ & ♀)	Setal Numbers on Internal Surface of Patella (by gender)
Hoffmannihadrurus gertschi	4.133–4.733 (4.507)	♀ 14–23 (18.50)
Hoffmannihadrurus aztecus	3.250–5.091 (4.032)	♂ 18–24 (19.67) ♀ 21–23 (22.00)
Hoffmannihadrurus	**3.250–5.091 (4.190) [12]**	♂ **18–24 (19.67) [8]** ♀ **14–23 (18.50) [4]**
Hadrurus hirsutus	10.0–11.0 (10.50)	♂ 26–35 (30.75)
Hadrurus concolorous	10.0–13.0 (11.119)	♂ 37–41 (39.00) ♀ 21–25 (23.00)
Hadrurus pinteri	10.0–12.0 (10.695)	♂ 41–49 (44.25) ♀ 28–41 (35.00)
Hadrurus arizonensis	9.857–11.0 (10.429)	♂ 51–58 (54.50) ♀ 32–33 (32.50)
Hadrurus obscurus	10.0–12.0 (11.067)	♂ 60–61 (60.50) ♀ 27–33 (30.25)
Hadrurus spadix	11.2–12.0 (11.5)	♂ 62–68 (65.00) ♀ 34–38 (36.00)
Hadrurus	**9.857–13.0 (10.959) [24]**	♂ **26–68 (45.75) [20]** ♀ **21–41 (31.71) [14]**
Mean Difference (%)	**162 %**	♂ **133 %** ♀ **71 %**

1.000). This character is inapplicable for the outgroup *Chaerilus* and family Iuridae because it only pertains to 10-carinae configurations (i.e., these taxa conform to the 8-carinae configuration). Rounded chelal palm with carinae *D1* and *E* carinae (state = 0) distribution is based on the optimization sequence, distributed for family Caraboctonidae if accelerated and subfamily Caraboctoninae if delayed. Similarly, vaulted chelal palm with rounded and coarsely granulated *D3* and *D4* carinae (state = 1) distributes for subfamily Hadrurinae if accelerated and genus *Hadrurus* if delayed. Vaulted chelal palm with discrete *D3* and *D4* carinae (state = 2) distributes consistently for genus *Hoffmannihadrurus*.

Williams (1970: 31–32) was the first to observe this difference between *Hoffmannihadrurus* and *Hadrurus*: "… It [referring both to *Hoffmannihadrurus aztecus* and *H. gertschi*, which at that time were combined] differs from all other *Hadrurus* species in the following … dorsal keels of pedipalp palm are narrower, tending to be more smooth than granular …" Figures 14–21 illustrate the *D3* and *D4* carinae of the pedipalp chela for all eight species comprising genera *Hoffmannihadrurus* and *Hadrurus*. Williams' (1970) observation is quite clear in these photographs: in *Hoffmannihadrurus*, *D3* and *D4* are well defined on the palm, though granular, not exhibiting a rounded appearance that is covered with coarse granulation. In addition, due to the clear delineation of these carinae basally, the intercarinal area is distinct, wide and devoid of granulation. In *Hadrurus*, these carinae basally are quite rounded, covered with coarse granulation, obscuring the intercarinal area, which is quite narrow where it is smooth.

Character 29: Development of ventrolateral (*VL*) and ventromedian (*VM*) carinae of sternite VII (**0:** *VL* and *VM* absent; **1:** *VL* present, *VM* smooth to vestigial; **2:** *VL* present, *VM* irregularly granulate to crenulate; **3:** *VL* present, *VM* absent); characteristics = (none | 3 | 1.000 | 1.000 | 1.000). Smooth to vestigial *VM* carinae (state = 1) is unambiguously distributed for superfamily Iuroidea. Granulate to crenulate *VM* carinae (state = 2) distribution is dependent on the optimization sequence, distributed for subfamily Hadrurinae if accelerated and distributed for genus *Hadrurus* if delayed. Obsolete *VM* carinae (state = 3) are consistently distributed for genus *Hoffmannihadrurus*.

Stahnke (1971: 125), in his redescription of *Hoffmannihadrurus aztecus*, wrote "… *Sternites* … seventh with one pair of lateral keels bearing rather large confluent granules …" Similarly, Williams (1970b: 9), when describing a composite *Hoffmannihadrurus aztecus*, wrote: "… Last sternite of mesosoma with single pair of keels, these lateral and granular …" Soleglad (1976: 123) wrote, in his description of *Hoffmannihadrurus gertschi*: "… One pair of weak, smooth keels on last sternite …" Williams (1970a: 171), in his redescription of *Hadrurus pinteri*, wrote: "… last sternite … with two pairs of incomplete granular lateral keels …" Stahnke (1969: 64) wrote, when describing *Hadrurus thayeri* (= *H. hirsutus*): "… Sternite … VII lightly granular and bearing two pair of lateral keels with confluent granules …" We checked all eight species of genera *Hoffmannihadrurus* and *Hadrurus* and can confirm the statements above: the ventromedian (*VM*) carinae of the last sternite in *Hoffmannihadrurus* are absent. In genus *Hadrurus*, they are present and are at least irregularly granulate; based on our observations, the most developed *VM* carinae are found in *H. pinteri*, *H. concolorous*, and *H. hirsutus*, while the weakest developed *VM* are found in *H. spadix* and *H. obscurus*.

Results: This completes the fundamental character set. We will now discuss the cladistic sequence that specifically deals with these characters. In Figure 22, we present a cladogram constructed from majority-rule consensus (also supported by semi-strict consensus) of three MPTs. The support data for this sequence are: steps/CI/RI/G-fit = 46/1.0/1.0/-22.0. Notice that there is no homoplasy present

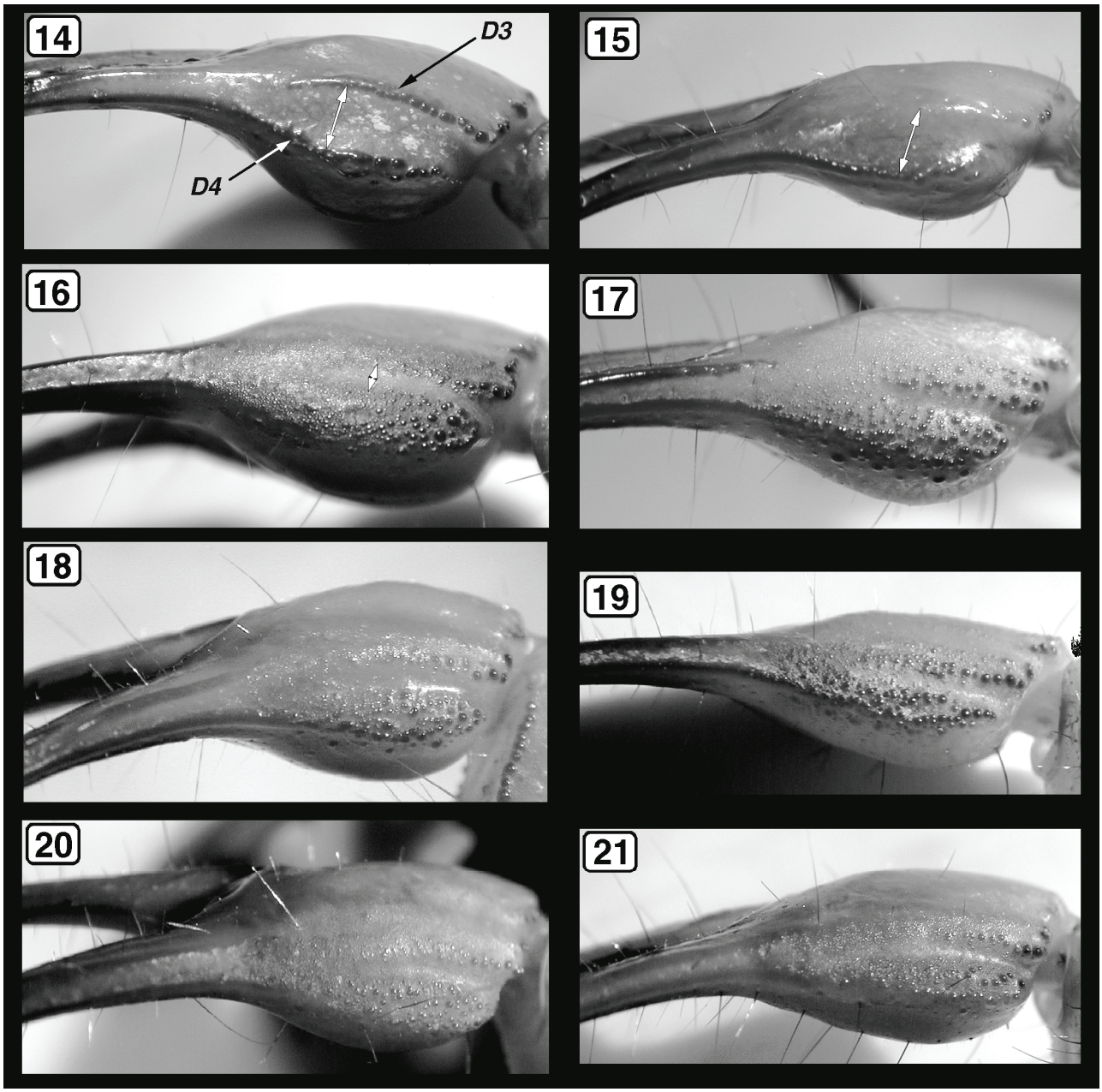

Fig. 14-21. Dorsoexternal view of pedipalp chelal palm showing the dorsosecondary (*D3*) and dorsomarginal (*D4*) carinae, and intercarinal area (double-headed *white arrow*). Note that carinae are discretely defined basally in *Hoffmannihadrurus*, the intercarinal area smooth and wide. In *Hadrurus*, these carinae are conspicuously rounded and coarsely covered with large granules, the intercarinal area narrow due to this granulation. **14.** *Hoffmannihadrurus gertschi*, female, Iguala, Guerrero, Mexico. **15.** *Hoffmannihadrurus aztecus*, female, Tehuacan, Puebla, Mexico. **16.** *Hadrurus pinteri*, female, Oakies Landing, Baja California, Mexico. **17.** *Hadrurus concolorous*, female, Santa Rosalia, Baja California Sur, Mexico. **18.** *Hadrurus hirsutus*, male, Cabo San Lucas, Baja California Sur, Mexico. **19.** *Hadrurus spadix*, female, Winnemucca, Humboldt Co., Nevada, USA. **20.** *Hadrurus obscurus*, female, Indian Gorge Canyon, ABDSP, California, USA. **21.** *Hadrurus arizonensis*, female, Carrizo Badlands, ABDSP, California, USA.

in this analysis. With these fundamental characters we were able to demonstrate monophyly of all taxonomic components of superfamily Iuroidea down to the genus level. We also conducted bootstrap/jackknife analyses of this sequence, their results are stated in Fig. 22. We see that genera *Hadrurus* and *Hoffmannihadrurus* were supported by 67/66 % of the 10,000 pseudoreplicates generated in the bootstrap/jackknife sequences. In contrast, for the bootstrap/jackknife analysis based on the data of Francke & Prendini's (2008) that we conducted in this study (Fig. 1), we see that any meaningful clade refinement did not go below that of subfamily, and the support for their result, "*gertschi* + *pinteri*" was only 44 %. Table I also compares the support for Francke & Prendini's (2008) two clades of interest to this analysis. In our fundamental character analysis, Francke & Prendini's (2008) clade "*gertschi* + *pinteri*" did not even register five percent support (the minimum support reported by PAUP).

In this analysis, the monophyly of genus *Hoffmannihadrurus* is supported by five unambiguous characters: character-11 (state = 2), trichobothrium *ib* placement; character-20 (state = 3), spinule cluster configuration of tarsus;

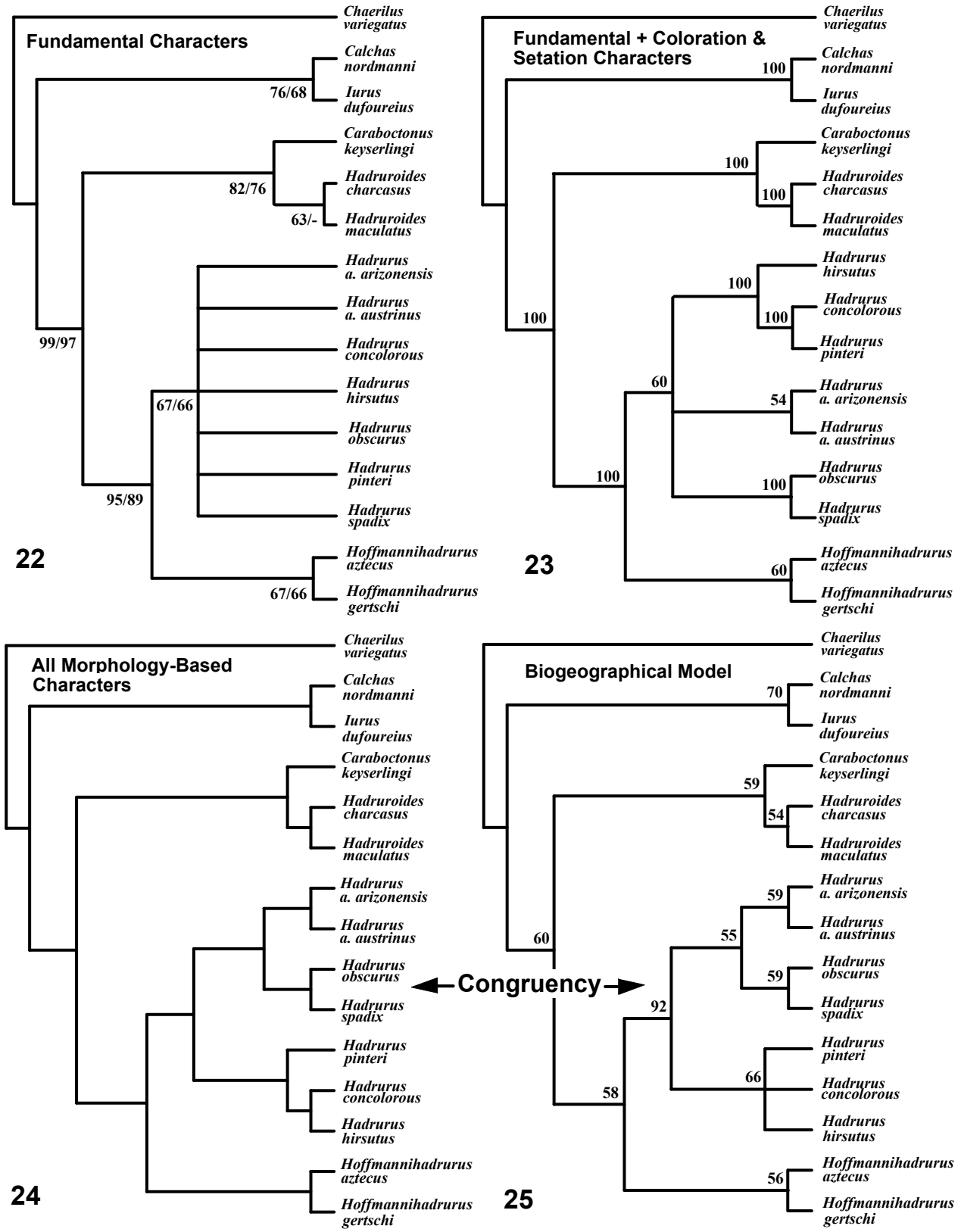

Fig. 22–25: Iuroidea, cladistic and biogeographic analyses. **22.** Cladogram based on fundamental characters (1–29) showing delineation of families, subfamilies and genera of superfamily Iuroidea. Cladogram constructed from majority-rule and semi-strict consensus of three MPTs with following support: steps/CI/RI/G-fit = 46/1.0/1.0/-22.0. Numbers below branches show mean value of five sequences of bootstrap/jackknife (1000 pseudoreplicates per) support of that node. **23.** Cladogram based on fundamental and lower level characters (1–37) of subfamily Hadrurinae involving setation and coloration. Cladogram constructed from majority-rule consensus of 35 MPTs with following support: steps/CI/RI/G-fit = 70/0.9714/0.9808/-29.500. Numbers above branches show perentage of 35 MPTs supporting that node. **24.** Cladogram based on all morphology-based characters (1–40), including accessory trichobothria loss hypothesis. See Fig. 26 for character distribution and bootstrap/jackknife support. **25.** Tree based on majority-rule consensus of 3638 MPTs showing biogeographic model with following support: steps/CI/RI/G-fit = 15/1.0/1.0/-5.0. Numbers above branches show perentage of 3638 MPTs supporting that node. Note that the tree based on a simple biogeographical model is congruent with the cladogram based on morphology in Fig. 24.

character-27 (state = 4), composition of patellar internal surface; character-28 (state = 2) chelal *D3* and *D4* carinae composition, and character-29 (state = 3), sternite VII *VM* carinae development. Clearly, we can reinstate genus *Hoffmannihadrurus* from the fundamental character set analysis alone.

(2) Low-level characters: coloration and setation

The low-level characters deal primarily with the phylogeny of subfamily Hadrurinae and its two genera, which were established through the cladistic analysis of the fundamental character set (see Fig. 22). In general, these characters refer to coloration and its patterns as well as localized setation. The unique aculear gland is also modeled in this character set. Since most of these characters deal specifically with Hadrurinae and are quite low-level in their taxonomic importance, polarity is not mapped upward into the sister subfamily Caraboctoninae, family Iuridae, or outgroup *Chaerilus*. We strongly suggest here that the evolution of subtle pigmentation found on metasomal carinae, a group of setae found on a segment surface, etc., is quite localized in taxonomic sense, possibly subject to strong selection due to animal's environment, and cannot be traced upwards into tribes, subfamilies, or families. Even tracing pigmentation trends between genera is nonsensical in many cases.

Character 30: Development of telson aculear glands (**0:** not present; **1:** present); characteristics = (see below | 1 | 1.000 | 1.000 | 1.000). This character is unambiguously distributed for the subfamily Hadrurinae as the presence of an aculear gland (state =1). This is a hypothesis: we observe aculear glands in both hadrurine genera and in two species of one major group of *Hadrurus* (species from Baja California peninsula). We hypothesize here that both genera inherited the aculear gland from their common ancestor, and then this gland was subsequently lost independently (see character 31). See Williams (1970b: fig. 10), Stahnke (1971: fig. 4), and Soleglad (1976: fig. 41) for information concerning the aculear gland.

Character 31: Aculear gland loss (**0:** not lost; **1:** lost; **-:** inapplicable); characteristics = (see below | 4 | 0.500 | 0.714 | 0.600). The loss of the aculear glands (state = 1) occurred independently three times, once for the clade "(*Hadrurus a. arizonensis* + *H. a. austrinus*) + (*H. obscurus* + *H. spadix*)", in *H. hirsutus*, and in *Hoffmannihadrurus gertschi*. Since these are clearly independent losses, we could have assigned three separate "gland lost" states, however, we opted to accept the homoplasy (i.e., CI = 0.500).

We will show below in the final cladistic analysis, when all morphology-based characters are considered (as shown in Fig. 26) and as augmented by observing the geographical distribution of Hadrurinae, that the loss of the telson aculear glands appears to be a more recent derivation, furthering supporting the hypothesis that the common ancestor of these two genera (i.e., common ancestor of subfamily Hadrurinae) exhibited these glands.

Character 32: Setation of pedipalp patella internal surface (**0:** irregular in number or reduced considerably in length; **1:** long stiff bristles, numbers range 18–24; **2:** long stiff bristles, numbers range 26–41; **3:** long stiff bristles, numbers range 41–49 ; **4:** long stiff bristles, numbers range 51–68; **-:** inapplicable); characteristics = (none | 5 | 1.000 | 1.000 | 1.000). We mapped the setal configuration for subfamily Caraboctoninae but considered the low-level nature of this character to be inapplicable for Iuridae and outgroup *Chaerilus*. Members of Caraboctoninae showed no consistency in this setation, from short setae to elongated setae occurring in large numbers to small numbers (state = 0). Members of Hadrurinae consistently exhibited stiff elongated setae on this surface, but differed significantly in their density. The character distribution of the setal number range breakdown for Hadrurinae is as follows: (state = 1) distribution is dependent on the optimization sequence, distributed for subfamily Hadrurinae if accelerated and genus *Hoffmannihadrurus* if delayed; (state = 2) distribution is also dependent on the optimization sequence, distributed for *Hadrurus* if accelerated and clade "*H. concolorous* + *H. hirsutus*" if delayed; (state = 3) consistently distributes for *H. pinteri*; and (state = 4) distributes consistently for clade "*H. arizonensis* + (*H. obscurus* + *H. spadix*)". Note that the setal number ranges are for adult males; see Table II for further statistics including both genders.

Stahnke (1945: 9) was the first to observe the differences in setation density in *Hoffmannihadrurus* and *Hadrurus* as he discussed five specimens of *Hoffmannihadrurus*, spanning both species, from Mexican states Oaxaca, Puebla, and Guerrero: "… Pedipalps: … with bristles weaker and less dense than *H. hirsutus* (= *H. arizonensis*) …" Figures 6–13 illustrate these observable differences in setation density of the inner surface of the pedipalp patella between *Hoffmannihadrurus* (Figs. 6–7) and *Hadrurus* (Figs. 8–13). As indicated by the distribution of this character, *Hadrurus concolorous* and *H. hirsutus* (Tab. II) have the least dense setation in *Hadrurus*, but considerably greater than that found in *Hoffmannihadrurus*, roughly 70 % greater in the adult male. Following is the mean difference percentage of these assemblages as modeled by the character states: *Hoffmannihadrurus* < (70 %) *H. hirsutus* + *H. concolorous* < (32 %) *H. pinteri* < (36 %) *H. arizonensis* + *H. obscurus* + *H. spadix*. The mean value difference between *Hoffmannihadrurus* and *Hadrurus* is 133 % in males.

It is interesting to note that in a series of *H. pinteri* specimens from Isla Danzante, Baja California Sur, Mexico, we encountered a very low setal count for the patella internal surface. We examined three adult females whose setal numbers ranged only 11–13. Williams (1970b) reported a similar reduction in setation of the dorsal carinae of the metasoma in island populations of *H. pinteri*: "… hirsuteness of dorsal keels on metasomal segments IV and V reduced to obsolescent …" We are currently studying this island population to see if other differences are present between it and mainland specimens (in progress).

Character 33: Setation of metasoma *VM* carinae (I–IV) (**0:** paired on *VM* carinae; **1:** irregular, but not located in intercarinal area; **2:** irregular, numerous setae located in intercarinal area: **-:** inapplicable); characteristics = (none | 4 | 0.750 | 0.833 | 0.750). We mapped the setal configuration for subfamily Caraboctoninae but considered the low-level nature of this character to be inapplicable for Iuridae and outgroup *Chaerilus*. Members of Caraboctoninae exhibited pairs of regularly placed setae located on the ventromedian (*VM*) carinae (state = 0). Members of Hadrurinae exhibited irregularly placed setae on the *VM* carinae across the species but the placement of setae in the intercarinal area is

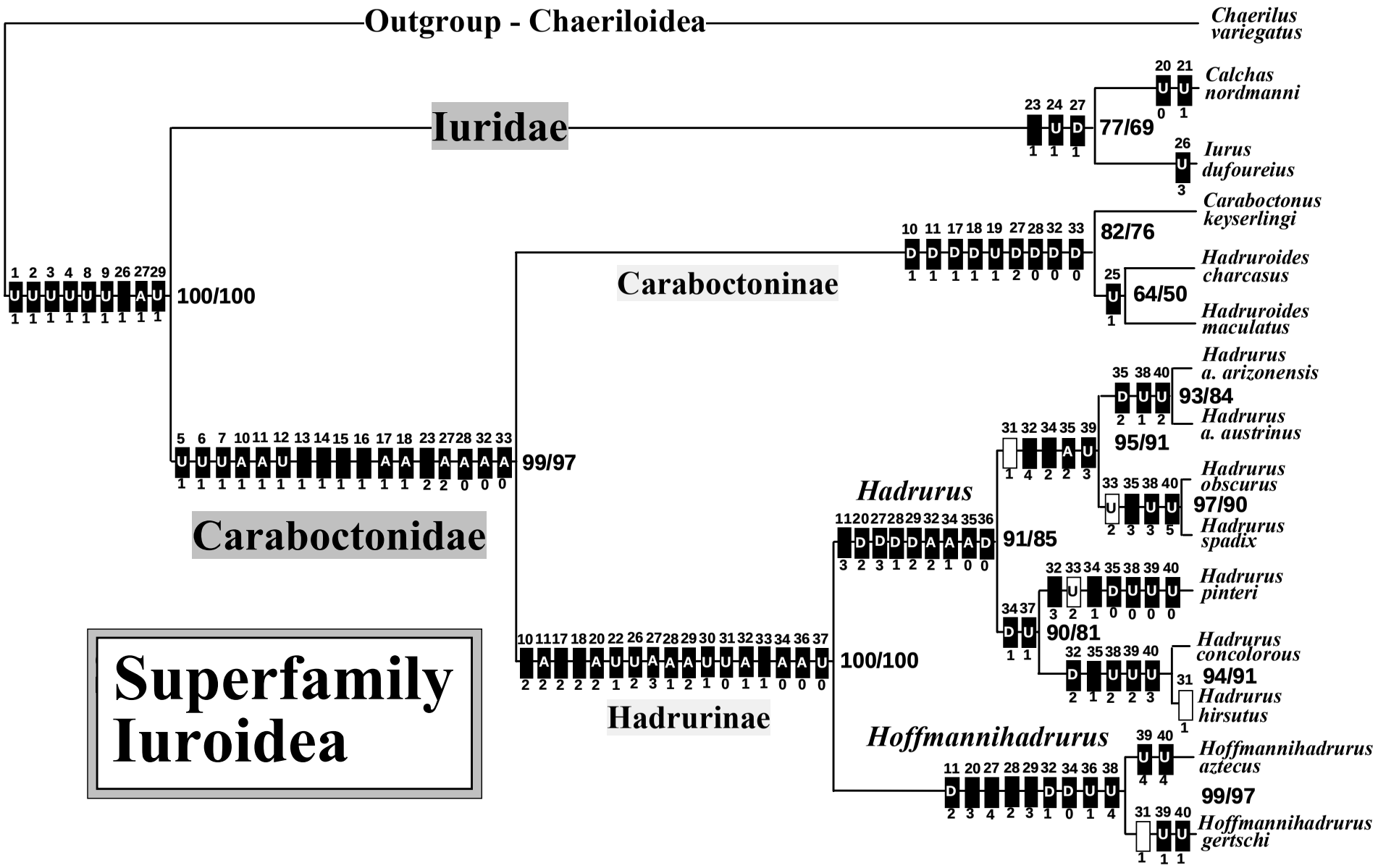

Fig. 26: Cladogram of superfamily Iuroidea showing distribution of morphology-based characters. Character number shown on top, character state on bottom; open rectangle depicts homoplasious character. "U" indicates unambiguous distribution, "A" indicates distributed ACCTRAN only, and "D" distributed DELTRAN only. Numbers inside node indicate bootstrap/jackknife mean value of five sequences of 10000 pseudoreplicates per algorithm. Note, uninformative characters (1–4, 8–9, and 21) are shown. Cladistic sequence generated a *single* MPT with the following support: steps/CI/RI/G-Fit = 105/0.9714/0.9812/-32.350.

variable as follows: the condition of lacking setae in intercarinal area (state = 1) distributes consistently for subfamily Hadrurinae; the condition of setae present in intercarinal area (state = 2) independently distributes unambiguously for *H. pinteri* and the clade "*H. obscurus* + *H. spadix*". This character, as mapped, demonstrates minor homoplasy (CI = 0.750).

Williams (1970a: 171; 1970b: 11, 17, 28) was the first to report the presence of setae in the *VM* intercarinal area for *H. pinteri*, *H. spadix*, and *H. obscurus*.

Character 34: General coloration and patterns on carapace and mesosoma (**0:** Carapace with pattern on posterior area, marginally reaching lateral eyes; mesosomal pattern covering all tergites, both patterns exhibiting no variability; **1:** Carapace with pattern on posterior area, but not reaching lateral eyes; mesosomal pattern variable, both patterns exhibiting variability; **2:** Carapace with pattern on posterior area connecting median tubercle and lateral eyes; mesosomal pattern variable, both patterns exhibiting variability; **-:** inapplicable); characteristics = (none | 3 | 1.000 | 1.000 | 1.000). We only mapped the coloration and patterns for Hadrurinae, considering the low-level nature of this character to be inapplicable for assemblages outside this subfamily (reasons given elsewhere). (state = 0) distribution is dependent on the optimization sequence, distributed for subfamily Hadrurinae if accelerated and genus *Hoffmannihadrurus* if delayed; (state = 1) distribution is also dependent on the optimization sequence, distributed for *Hadrurus* if accelerated and the clade "*H. pinteri* + *H. concolorous* + *H. hirsutus*" if delayed; (state = 2) distributes consistently for clade "*H. arizonensis* + *H. spadix* + *H. obscurus*".

Fet *et al*. (2001: figs. 2–12) were the first to quantify, in a cladistic sense, the carapace and mesosomal coloration patterns in five species of *Hadrurus*. Of particular importance, they pointed out the symmetry between clades "*H. arizonensis* subspecies", "*H. spadix* + *H. obscurus*", and "*H. hirsutus* + *H. concolorous*" where all three exhibited consistency of the anterior pattern on the carapace, but great variability was present on the posterior region of carapace as well as on the mesosoma. They therefore concluded that the pattern surrounding the interocular area of the carapace was of taxonomic importance, while the other patterns were of little importance. Based on this analysis by Fet *et al*. (2001) and our new analysis of additional material, in particular *Hoffmannihadrurus* and *Hadrurus pinteri*, we see that the carapacial pattern exhibited in *Hoffmannihadrurus aztecus* is visible in *H. gertschi* as well, but it is difficult to discern due to the overall pigmentation uniformly covering the carapace, mesosoma, metasoma, and telson in *H. gertschi*. Both the posterior half of the carapace and the entire mesosoma are darker than the anterior region of the carapace, as observed by both Williams (1970b: 9) and Soleglad (1976: 123). Both *Hoffmannihadrurus aztecus* and *H. gertschi* have conspicuous reddish pigmentation on the ventral carinae of the metasoma (see character 36 below). For *Hadrurus pinteri*, we see an entirely different configuration of patterns. The carapace and mesosoma are covered with a slightly variable, somewhat marbled melanic pattern, the anterior edge of the carapace being lighter than the posterior half. The metasoma is also covered with a somewhat lighter, also marbled, melanic pattern, with segment V darker than the other segments (see character 37 below), as reported by Williams (1970a: 170–171). The telson is lighter than the metasomal segments, and pedipalp chelae are slightly darker than pedipalp patella and femur, adding to the somewhat spectacular coloration of this species, particularly clear in Stahnke's (1969: fig. 2) photograph of a subadult specimen. We can conclude here that *Hoffmannihadrurus gertschi* is uniformly darker on the carapace (with anterior area lighter), mesosoma, pedipalps, metasoma, and telson. The melanic pattern of the carapace and mesosoma as seen in *H. aztecus* occurs also in *H. gertschi*, thus making these areas even darker in color. In contrast, *Hadrurus pinteri* is not uniformly darker, its darker patterns are marbled in places, metasomal segment V is darker than the other segments, telson is lighter than the metasoma, pedipalp chelae darker than its other segments, which clearly is not a pattern that is homologous to that seen in *Hoffmannihadrurus gertschi*. It is also important to point out that Williams (1970b: 16–17) wrote "… *Hadrurus concolorous* occupies a wide variety of habitat situations … has become a variable species … light phases, dark phases, and all degrees of intermediates occur …" Since *H. pinteri* occupies a single microhabitat (i.e., volcanic), it is not unreasonable to suggest that its bizarre pigmentation patterns are due to the selection for this preferred habitat, and thus a localized derivation for this species.

Therefore, in our opinion, the attempts of Francke & Prendini (2008) to equate the coloration and its patterns of *Hoffmannihadrurus gertschi* with that of *Hadrurus pinteri*, are quite superficial. Interestingly (as discussed elsewhere), out of the eight coloration and pattern characters proposed by Francke & Prendini (2008), the clade "*Hoffmannihadrurus gertschi* + *Hadrurus pinteri*" agreed in six of these characters, two exclusively. As demonstrated in this paper, these characters alone already yield Francke & Prendini's result that the abovementioned clade was monophyletic, thus providing them with a reason for synonymizing genus *Hoffmannihadrurus*.

Character 35: Specific carapace and mesosoma coloration (**0:** interocular area marbled, darker pattern not reaching lateral eyes; **1:** interocular area not marbled, darker pattern not reaching lateral eyes; **2:** interocular area not marbled, pattern reaching lateral eyes is crescent-shaped; **3:** interocular area not marbled, pattern reaching lateral eyes is wedge-shape; **-:** inapplicable); characteristics = (none | 4 | 1.000 | 1.000 | 1.000). For this character, we further refine the taxa complying with states 1–2 of character 34. Therefore, other taxa are coded as inapplicable. (state = 0) distribution is dependent on the optimization sequence, distributed for *Hadrurus* if accelerated and for *H. pinteri* if delayed; (state = 1) distributes consistently for clade "*H. concolorous* + *H. hirsutus*"; (state = 2) distribution is dependent on the optimization sequence, distributed for clade "*H. arizonensis* + *H. obscurus* + *H. spadix*" if accelerated and for *H. arizonensis* if delayed; (state = 3) distributes consistently for clade "*H. obscurus* + *H. spadix*".

This character further refines the pattern of the interocular area of the carapace and is based primarily on the analysis presented in Fet *et al*. (2001). Again, as stated above, the pattern occurring in this area is consistent within these clades, and therefore is deemed taxonomically important.

Character 36: Metasoma ventrolateral (*VL*) and (*VM*) carinae coloration, segments I–IV (**0:** no pigment; **1:** outlined in

red pigment; **-:** inapplicable); characteristics = (none | 2 | 1.000 | 1.000 | 1.000). We only mapped the coloration and its patterns for Hadrurinae, considering the low-level nature of this character to be inapplicable for assemblages outside this subfamily. Nonpigmented *VM* carinae (state = 0) distribution is dependent on the optimization sequence, distributed for subfamily Hadrurinae if accelerated and *Hadrurus* if delayed; pigmented *VM* carinae condition (state = 1) is unambiguously distributed for genus *Hoffmannihadrurus*.

The pigmented ventral carinae of the metasoma of *Hoffmannihadrurus* were first pointed out by Williams (1970b: fig. 11), and further quantified by Soleglad (1976: table 4) for both species of *Hoffmannihadrurus*. Stahnke (1971: 122), in his redescription of the *H. aztecus* type, did not detect this pigmentation. However, we have noted that in several specimens of *H. aztecus* viewed by us the faint pigmentation has faded due to many years of preservation. In contrast, the pigmentation in *H. gertschi*, which is much darker, is still visible in examined specimens. We suspect that, due to the overall dark pigmentation in *H. gertschi* (see discussion above), the ventral carinae pigmentation is more exaggerated.

Francke & Prendini (2008), as discussed elsewhere in this paper, mapped the pigmented *VM* carinae to subfamily Caraboctoninae, where they coded both genera (two species) with a state of "pigmented". We strongly suggest that the evolution of such low-level character as coloration of metasomal carinae cannot and should not be analyzed across subfamilies, especially subfamilies exhibiting significant geographic disjunctions. As discussed elsewhere, we examined the ventral carinal pigmentation in three caraboctonine species and determined that it was essentially absent in the dark scorpion *Caraboctonus* and was present in two species of *Hadruroides*. However, in *Hadruroides*, all metasomal carinae, ventral, lateral, and dorsal, are pigmented if they are granulate, vestigial carinae not exhibiting pigmentation. In *H. maculatus*, only the setal pairs were pigmented with small circumventing patterns, since the *VM* carinae were essentially obsolete. In *Hoffmannihadrurus*, carinae pigmentation is exclusively found on the ventral carinae, vestigial, smooth, or otherwise.

Character 37: Metasomal segment V pigmentation with respect to other segments (**0:** same pigmentation level as other segments; **1:** segment darker than other segments; -: inapplicable); characteristics = (none | 2 | 1.000 | 1.000 | 1.000). (state = 0), segment V same color as other segments, distributes unambiguously for subfamily Hadrurinae, and similarly (state = 1), segment V darker than other segments, distributes unambiguously for clade "*H. pinteri* + *H. concolorous* + *H. hirsutus*".

Stahnke (1969: 63) and Williams (1970a, 1970b) were the first to address this character for these three *Hadrurus* species.

Results: This completes the low-level character set. We will now discuss the cladistic sequence that specifically deals with these characters as they augment the fundamental character set (characters 1–37). In Figure 23, we present a cladogram constructed from majority-rule consensus of 35 MPTs with the following support: steps/CI/RI/G-fit = 70/0.9714/0.9808/-29.500. In this analysis, we see major clades forming in genus *Hadrurus*, such as "*H. pinteri* + *H. concolorous* + *H. hirsutus*" and "*H. obscurus* + *H. spadix*". Table I shows that the bootstrap/jackknife support for *Hoffmannihadrurus* has increased with the addition of these eight low-level characters. At the same time, just as with the fundamental character cladistic result, the support for Francke & Prendini's (2008) clade "*Hoffmannihadrurus gertschi* + *Hadrurus pinteri*" was below 5 % (i.e., did not register with either bootstrap or jackknife algorithms). Finally, we might add here that the only "assumption" enforced in these 37 characters was the aculear gland loss hypothesis. However, whether we assume aculear gland gain or loss, both involve three independent derivations; therefore this hypothesis has no effect on the topological result or its overall support. See discussion on accessory trichobothria loss and biogeographic issues, which supports the gland loss hypothesis.

(3) Accessory trichobothria loss hypothesis

Soleglad & Fet (2004: 102–105) presented an original hypothesis of "accessory trichobothria loss" based on the data collected from three diverse scorpion groups that exhibited significant neobothriotaxy: *Anuroctonus* (Uroctoninae, Chactidae), the subject of their study, 900+ samples; *Euscorpius* (Euscorpiinae, Euscorpiidae), 1500+ samples; and Hadrurinae, 600+ samples. Since this analysis is still ongoing, the number of samples by now has increased considerably (*Anuroctonus*, 1200+ samples; *Euscorpius*, 7000+ samples; and Hadrurinae, 690+ samples). A sample represents a single pedipalp; in most cases, both pedipalps were examined for each scorpion specimen.

Based on simple observations of statistical data on the number of accessory trichobothria found in a scorpion group with major neobothriotaxy, it is clear that in almost all cases (chactid subfamilies Chactinae and Brotheinae being notable exceptions) the number within a particular trichobothrial series is variable. Our hypothesis suggests that variation in these accessory trichobothria numbers, although high, is not random, but instead shows consistency within taxonomic aggregates as well as across their geographic ranges. This, in turn, provides us with potential diagnostic characters for further diagnosing these aggregates. As a hypothesis based on these data and the analysis discussed below, we further suggest that the observed variation in chelal trichobothrial numbers is due to the *loss of accessory trichobothria* connected with *speciation* and *dispersal* within a species. This hypothetical dynamics could be interpreted in genetic terms of additive allele frequency variation and its impoverishment toward the periphery of a species' range, with an asymmetric gene flow. Although genetic mechanisms controlling scorpion trichobothria are unknown, such a hypothesis is consistent with the current knowledge of quantitative inheritance mechanisms for arthropod sensory setae, a well-studied model for quantitative inheritance in general (*Drosophila* bristles; Mackay, 1996, 2001). A significant statistical data exist on geographic distribution of accessory trichobothria supporting this hypothesis (see Soleglad & Fet, 2004) at least in three unrelated genera (*Anuroctonus*, *Euscorpius*, and *Hadrurus*). It must be noted here that a powerful corollary results from our hypothesis of accessory trichobothria *loss* (i.e., not *gain*) — we predict that for any group of closely related taxa exhibiting variable neobothriotaxy, the taxon

with the largest number of accessory trichobothria is presumably the most ancestral member of that group, i.e. the closest to the ancestral neobothriotaxic condition not affected by the number reduction. The likelihood of this corollary is quite evident in the discussion of accessory trichobothria loss discussed below for *Hadrurus*. We now highlight some of the more salient results presented in Soleglad & Fet (2004), as well as provide new data. Figure 27 shows a plot, by examined populations, of the number of accessory trichobothria for all six species. This includes the internal and ventral accessory trichobothria, and, if applicable, external accessory trichobothria.

In *Hadrurus arizonensis* where the numbers of the internal accessory trichobothria are relatively high, we observe significant and *consistent* differences in their numbers based on populations throughout western United States, Baja California, and Sonora, Mexico. Populations from northern Sonora exhibit the highest numbers in this series, and, following an east to west direction, we see that populations from northern Baja California and extreme southern California (with ABDSP the most western edge) to Picacho on the Colorado River exhibit the second highest numbers. Following northward in California to Riverside County, as well as into central Arizona, we see the number of trichobothria showing a reduction from the northern Sonoran population of 11.05% (Riverside) and 7.40% (Arizona). The most southern population of *H. a. arizonensis*, found in Guaymas, Sonora, exhibits double digit percentage drop in trichobothria numbers, 18.16%. The subspecies *H. a. austrinus*, which represents the most southern range of *H. arizonensis* in Baja California, also exhibits considerable reduction in trichobothria, 19.94%.

It is interesting to point out that the percentage of loss in accessory trichobothria is more significant in the internal series than in the ventral series for these species of *Hadrurus*, although the number of accessory trichobothria in the internal series is much lower than that in the ventral series, namely 2–6 internal (across all six species) versus 11–22 ventral. This implies that the stability of the internal series is much more affected by asymmetric gene flow during geographic dispersal and speciation than the ventral series. Two other conditions support this observation: (1) the accessory trichobothria in the internal series are in general petite in size, especially the more basal trichobothria, implying that trichobothria are in the process of being lost, a suggestion originally proposed by Soleglad & Fet (2001: Appendix A) (also see our Fig. 5); and (2) internal accessory trichobothria are absent altogether in *Hadrurus*'s sister genus *Hoffmannihadrurus* Fet & Soleglad, which we consider a synapomorphy for this genus.

In *Hadrurus*'s "spadix complex" (i.e., "*H. spadix* + *H. obscurus*", see Fet *et al*., 2001), we see a reduction in the internal trichobothrial series of the chela in *H. spadix* when compared to *H. obscurus*, exhibiting 27.77% drop in trichobothria (i.e., from three accessory trichobothria to two). We suggest here that the reduction in internal accessory trichobothria shown in *H. spadix* is a derivation of this species, thus a product of speciation. This suggestion is further supported by the range expansion seen in *H. spadix*, which is found as far north as Idaho and Oregon (see map in Fig. 28), whereas *H. obscurus* is restricted to southern and central California, occurring sympatrically in ABDSP with *H. a. arizonensis* (though occupying different microhabitats, i.e. not syntopic). Reduction in chelal trichobothria between the two species complexes exhibits significant differences of 55.90/21.21% (internal/ventral accessory trichobothria), the "arizonensis complex" (i.e., two subspecies of *H. arizonensis*) having the larger numbers. Since these two complexes form a monophyletic clade (as demonstrated in this paper, Fig. 26), we propose here that this significant loss of accessory trichobothria is a synapomorphy for the "spadix complex".

In the "hirsutus complex" (i.e., "*H. concolorous* + *H. hirsutus*") we see similar consistent reductions in the ventral trichobothria for *H. concolorous*. The population from Santa Rosalia, Baja California Sur, exhibits the largest ventral trichobothrial count, but this number is reduced in populations both in a northern and southern direction from Santa Rosalia. Specimens from the more northern Las Bombas exhibited 8.69% reduction in ventral trichobothria, and those from the more southern Los Aripes, showed a 6.36% reduction. The slight differences in internal trichobothria numbers for these five populations did not demonstrate any consistent trend, exhibiting differences of 1.21% to 8.52% between adjacent populations. For *H. concolorous* and *H. hirsutus*, we observe drops in the latter for both the internal and ventral chelal trichobothria series, exhibiting 2.82/13.53% difference. The significant lost of ventral trichobothria is considered a derivation in *H. hirsutus*, whose range is somewhat restricted to the Cape region of Baja California Sur. The external accessory trichobothria found in these two species also demonstrate a difference of 17.12% with *H. hirsutus* generally having only one accessory trichobothrium. Again, these losses in accessory trichobothria in all three series, the ventral, internal, and external, all found in *H. hirsutus*, indicate that this species is more derived than *H. concolorous*, possibly due to its geographic isolation in the Cape region of Baja California Sur. The loss of the aculear gland (as hypothesized in this paper) and the reduction of pectinal tooth counts (*H. hirsutus* has 17–22 % less teeth than *H. concolorous*) also support this conclusion.

In Figure 27, we see notable differences in the numbers of accessory trichobothria in all three series for *H. pinteri* in the two disjunctions of its range, the northern range with 5.13/9.81/12.50% reductions. But it must be stressed here that the samples from the southern disjunction are quite small, and we are in the process (in progress) of studying additional material from the southern disjunction and adjacent islands in Baja California Sur.

For genus *Hoffmannihadrurus* (species found in southern Mexico, not shown in Fig. 27, see map in Fig. 28), we see a drastic difference in the number of ventral accessory trichobothria: *H. aztecus* has 18.52% lower number than *H. gertschi*. Common to both, and a synapomorphy for the genus, is the absence of internal accessory trichobothria. However, *H. gertschi* has 3–4 external accessory trichobothria on the chelal palm, which are absent in *H. aztecus*.

Based on the presence of accessory trichobothria on the chela and the overwhelming evidence supporting loss of these trichobothria during speciation and species dispersal, we can assume that *Hadrurus pinteri* and *Hoffmannihadrurus gertschi*, the two species, in general, with the largest number of accessory trichobothria, are the most primitive

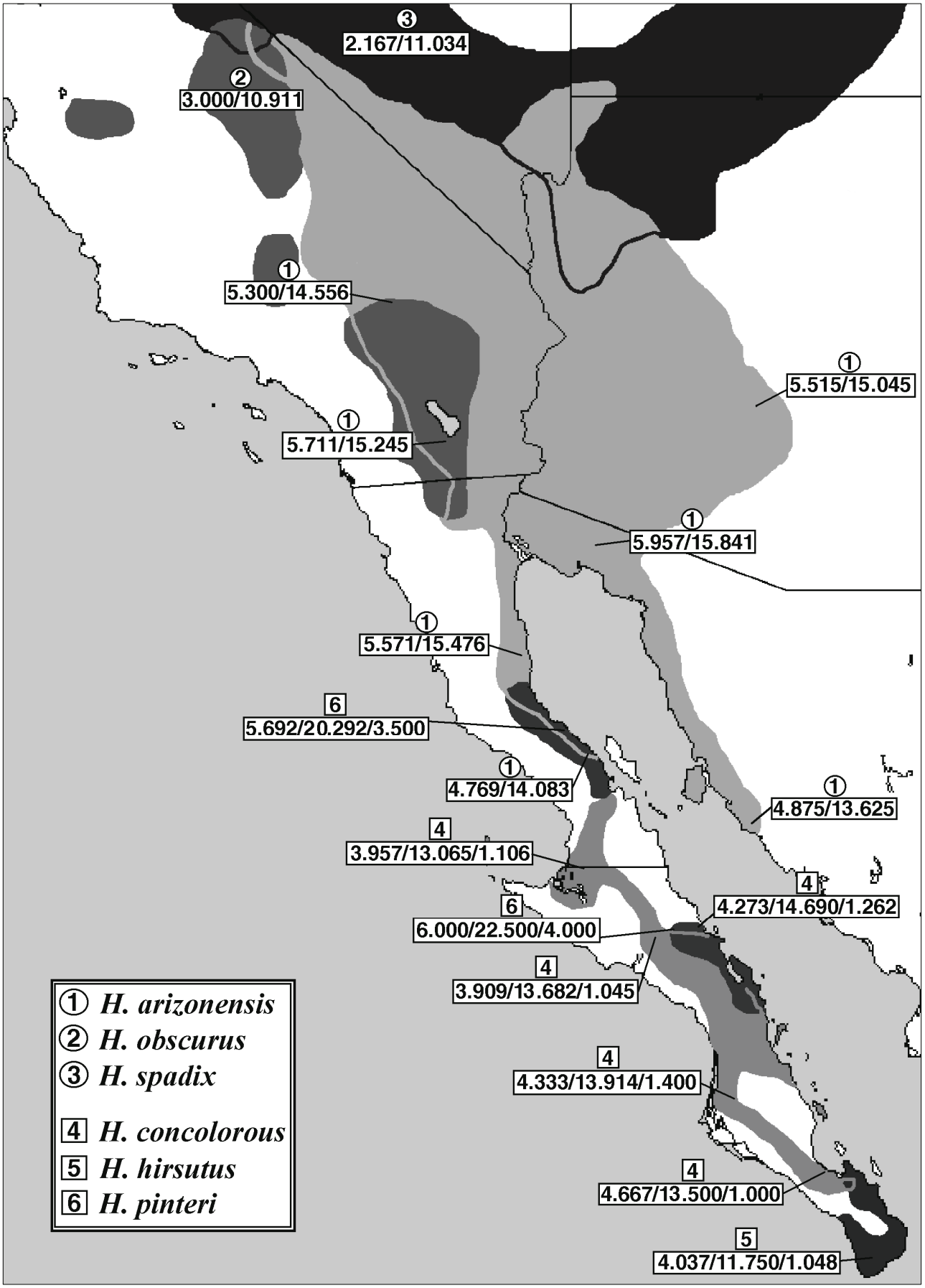

Fig. 27: Plots of the number of accessory trichobothria in *Hadrurus* based on populations. The data (i/v/e) is from Soleglad & Fet (2004: tab. VII), in part, and is based on 594 (internal), 576 (ventral), and 178 (external) samples (a sample is a single pedipalp). The statistics for *H. obscurus* and *H. spadix* are based on all samples examined, and therefore the rectangles indicating these data do not refer to a particular population. Note that external accessory trichobothria are limited to *H. concolorous*, *H. hirsutus*, and *H. pinteri*.

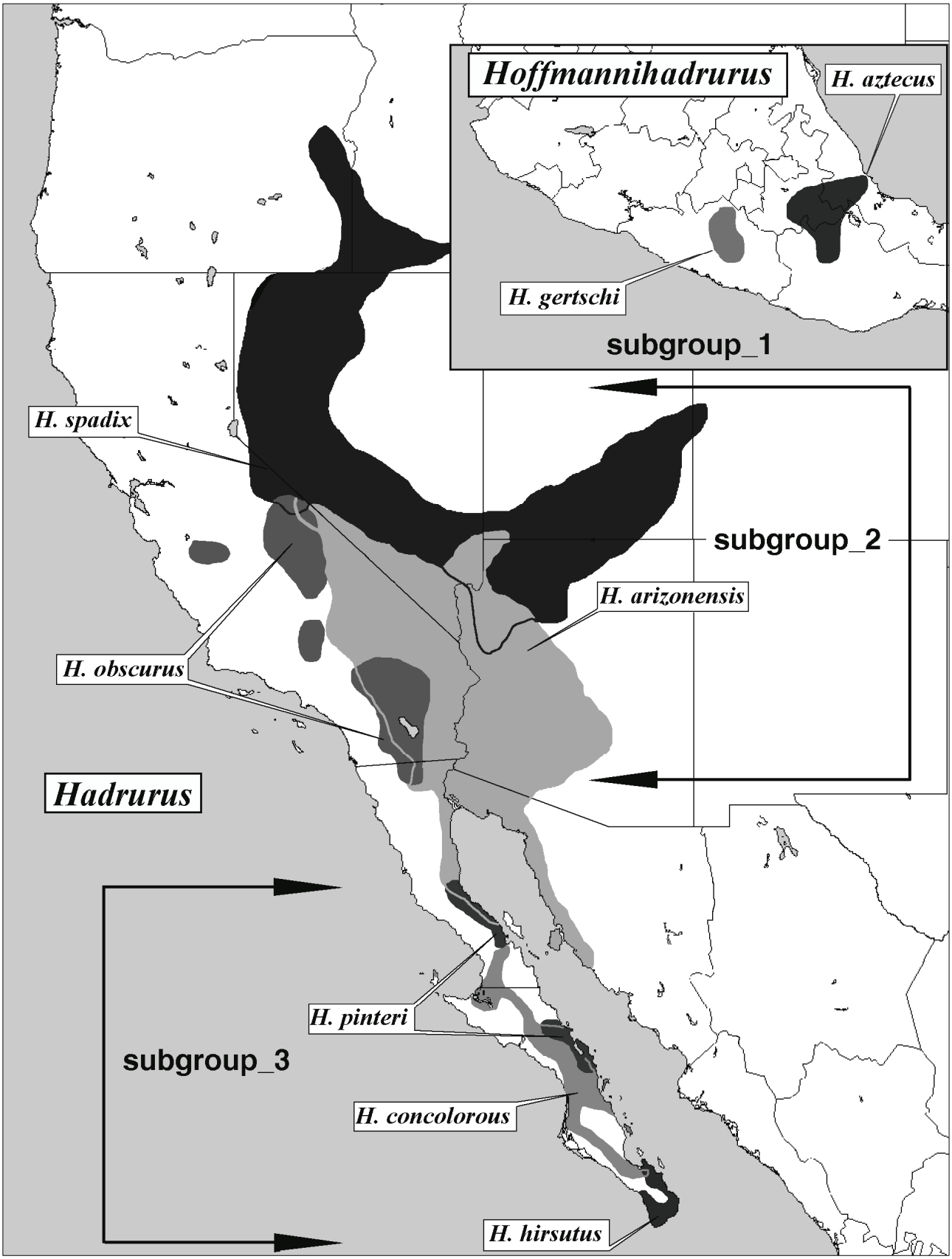

Fig. 28: Distribution of subfamily Hadrurinae in North America. Main map shows distribution of genus *Hadrurus* and insert shows distribution of *Hoffmannihadrurus* in southern Mexican states of Guerrero (*H. gertschi*), Puebla, Oaxaca, and Veracruz (*H. aztecus*). Overlapping distributions are indicated by thin polygonal lines. Subgroup designations based on Williams (1970b) phylogeny. Distributions based on specimens examined and from Gertsch & Allred (1965), Johnson & Allred (1972), Anderson (1975), Williams (1970b, 1980), and personal records from Matthew R. Graham and Graeme Lowe.

species within their respective genera (the corollary of our accessory trichobothria loss hypothesis). The attempt by Francke & Prendini (2008) to couple these two species by establishing no less than three trichobothria-based characters for this purpose is refuted here. The "synapomorphies" these authors attempted to establish, in our opinion, are symplesiomorphies inherited from the common ancestor of *Hadrurus* and *Hoffmannihadrurus*.

We represent the accessory trichobothria loss hypothesis described above with three characters modeling reductions on the chelal internal, external, and ventral surfaces. These three characters are partially ordered using PAUP user-tree definitions. This ordering parallels the accessory trichobothria-loss hypothesis described above. In addition, the creation of two or more different state-values is necessitated by this hypothesis which is supported, in part, by the topology shown in Fig. 23.

Character 38: Chelal internal accessory (*ia*) trichobothria loss (**0:** no loss, 5–6 *ia* present; **1:** no loss, 5–6 *ia* present; **2:** small loss, 3–5 *ia* present; **3:** large loss, 2–3 *ia* present; **4:** all *ia* lost; **-:** inapplicable); characteristics = (TREE = (-, 4, (0, (2)), (1, (3))) | 10 | 1.000 | 1.000 | 1.000). Modeling of accessory trichobothria loss is only applicable to subfamily Hadrurinae thus other taxa are coded inapplicable. All character states are distributed unambiguously as follows: (state = 0) for *Hadrurus pinteri*; (state = 1) for *H. arizonensis*; (state = 2) for clade "*H. concolorous* + *H. hirsutus*"; (state = 3) for clade "*H. obscurus* + *H. spadix*"; and (state = 4) for *Hoffmannihadrurus*.

Note that in this modeling we entertain two state values for "no loss" of *ia* trichobothria, a consequence of our accessory trichobothria loss hypothesis, see above.

Character 39: Chelal external accessory (*ea*) trichobothria loss (**0:** no loss, 3–4 *ea* present plus one *ea* on fixed finger; **1:** 3–4 *ea* present, *ea* on fixed finger lost; **2:** medium loss, 1–2 *ea* present; **3:** all *ea* lost; **4:** all *ea* lost; -: inapplicable); characteristics = (TREE = (-, (0, (2), 0, (3)), (1, (4))) | 11 | 1.000 | 1.000 | 1.000). Modeling of accessory trichobothria loss is only applicable to subfamily Hadrurinae thus other taxa are coded inapplicable. All character states are distributed unambiguously as follows: (state = 0) for *Hadrurus pinteri*; (state = 1) for *Hoffmannihadrurus gertschi*; (state = 2) for clade "*Hadrurus concolorous* + *H. hirsutus*"; (state = 3) for clade "*H. arizonensis* + *H. obscurus* + *H. spadix*"; and (state = 4) for *Hoffmannihadrurus aztecus*.

Note that in this modeling we entertain two state values for "all lost" of *ea* trichobothria, a consequence of our accessory trichobothria loss hypothesis, see above.

Character 40: Chelal ventral accessory (*va*) trichobothria loss (**0:** no loss, 16–22 *va* present; **1:** no loss, 16–22 *va* present; **2:** minor loss, 14–16 *va* present; **3:** medium loss, 11–15 *va* present; **4:** medium loss, 11–15 *va* present; **5:** significant loss, 10–12 *va* present; **-:** inapplicable); characteristics = (TREE = (-, (0, (3), 0, (2, (5))), (1, (4))) | 13 | 1.000 | 1.000 | 1.000). Modeling of accessory trichobothria loss is only applicable to subfamily Hadrurinae thus other taxa are coded inapplicable. All character states are distributed unambiguously as follows: (state = 0) for *Hadrurus pinteri*; (state = 1) for *Hoffmannihadrurus gertschi*; (state = 2) for *H. arizonensis*; (state = 3) for clade "*H. concolorous* + *H. hirsutus*"; (state = 4) for *Hoffmannihadrurus aztecus*; and (state = 5) for clade "*Hadrurus obscurus* + *H. spadix*".

As with the previous two characters, this modeling entertains two state values for "no loss" and "medium loss" of *va* trichobothria, a consequence of our accessory trichobothria loss hypothesis, see above.

Result: This completes all morphology-based characters, 1–40. In Figures 24 and 26 we present cladograms based on a single MPT with the following support: steps/CI/RI/G-Fit = 105/0.9714/0.9812/-32.350. In Fig. 26 we provide the bootstrap/jackknife support data (based on the mean of five sequences of 10,000 pseudoreplicates, a total of 50,000 per algorithm), showing at least 84 % support for all clades in subfamily Hadrurinae. For completeness and comparison with the other three analyses presented in this paper (Table I), as well as that of Francke & Prendini (2008), we note that genus *Hoffmannihadrurus* is supported 96–98 % (based on a smaller number of pseudoreplicates than that shown in Fig. 26). And again, Francke & Prendini's (2008) result, "*gertschi* + *pinteri*" does not register a minimal 5 %.

In summary, this total analysis based on all characters exhibited homoplasy in only two characters (31 and 33), 33 characters were informative, each node was supported by at least one consistently distributed character, and most were supported by one or more unambiguously distributed characters. All seven uninformative characters occurred in the fundamental character set; six are uninformative since they are autapomorphic for our outgroup taxon *Chaerilus variegatus*. The seventh uninformative character (presence of a tibial spur) is autapomorphic for *Calchas nordmanni.*

Weighting. We exercised implied (GOLOBOFF mode in PAUP) and successive (REWEIGHT in PAUP) weighting sequences against this final character data matrix (see Table III). For implied weighting, all six concavity constant values were applied (i.e., 0–5, the lower number having the most impact on homoplasious character weights) and for successive weighting, we initiated three nested sequences. All nine resulting trees, six from implied weighting and three from successive weighting, were identical to the single MPT generated with equal weighting. Although we could make the same claim as Francke & Prendini (2008), that "*eight* independent analyses of the morphological character matrix, under weighting regimes that minimized length as well as those that maximized fit, each located a single most parsimonious tree", we will state here that, with the low homoplasy exhibited in our final analysis, this result involving weighting is totally predictable and therefore is of no significance.

Constrained analysis. We forced a PAUP sequence using Francke & Prendini's (2008: fig. 4) resulting topology against our data matrix (Table III). Predictively, the support for this topology was considerably less than that obtained from a non-constrained sequence which resulted in our topology as shown in Fig. 26 (see Table IV). As shown in Table IV the consistency index is 13.3 % lower in the constrained analysis where no less than 13 out of the 33 informative characters exhibited homoplasy (in our analysis two characters are homoplasious). The CI of these characters (11, 20, 27–29, 31, 33–34, 36–40) ranged from 0.500 to 0.800, averaging 0.748. Curiously, five of these homoplasious characters, 11, 20, and 27–29, were fundamental characters. Of interest here, character 11 deals with the relative

Table III. Data matrix for cladistic analysis of superfamily Iuroidea. The seven uninformative characters are shown white on black.

	1234567890	1111111111 0123456789	2222222222 0123456789	3333333333 0123456789	4 0
Chaerilus variegatus	000000000	000------0	-0000000-0	0---------	-
Calchas nordmanni	111100011	0000000000	01011011-1	0---------	-
Iurus dufoureius	111100011	0000000000	10011031-1	0---------	-
Caraboctonus keyserlingi	111111111	1111111111	1002001201	0-00------	-
Hadruroides charcasus	111111111	1111111111	1002011201	0-00------	-
Hadruroides maculatus	111111111	1111111111	1002011201	0-00------	-
Hadrurus a. arizonensis	111111111	2311111220	2012002312	1141220013	2
Hadrurus a. austrinus	111111111	2311111220	2012002312	1141220013	2
Hadrurus concolorous	111111111	2311111220	2012002312	1021110122	3
Hadrurus hirsutus	111111111	2311111220	2012002312	1121110122	3
Hadrurus obscurus	111111111	2311111220	2012002312	1142230033	5
Hadrurus pinteri	111111111	2311111220	2012002312	1032100100	0
Hadrurus spadix	111111111	2311111220	2012002312	1142230033	5
Hoffmannihadrurus aztecus	111111111	2211111220	3012002423	10110-1044	4
Hoffmannihadrurus gertschi	111111111	2211111220	3012002423	11110-1041	1

Table IV. Comparison of support of new analysis presented in this paper with the constrained topology analysis of Francke & Prendini (2008).

	Steps	CI	RI	G-Fit
New Analysis	105	0.9714	0.9812	-32.350
Francke & Prendini (2008) Topology Constrained	119	0.8571	0.8938	-29.150
% delta	+13.3	-13.3	-9.8	-11.0

position of chelal trichobothrium *ib*, clearly misrepresented in Francke & Prendini's (2008) analysis, as discussed in detail in this paper. Character 20 specifies the four states of the spinule cluster attribute (type 3) exclusively found in superfamily Iuroidea. In this case, the homoplasy involves the degree of fusion of the spinule clusters. Note that a similar character in Francke & Prendini's (2008) analysis was also homoplasious, independently observed in *Hoffmannihadrurus aztecus* and *H. gertschi* (their character 49). The homoplasy in these two characters is indicative of the many problems in Francke & Prendini's (2008) analysis.

Biogeographic Considerations

As a historical observation, it has to be noted that already Williams (1970b: 31–32) defined three phylogenetic subgroups of genus *Hadrurus* based on morphology. These subgroups also happened to inhabit distinct geographical areas. As a separate subgroup, Williams (1970b) recognized *Hoffmannihadrurus aztecus* (known then as *Hadrurus aztecus*) from southern mainland Mexico stating "… this species appears to be only distantly related to the other species of the genus …" This observation is certainly supported by our study. The second subgroup of Williams (1970b) was composed of *H. arizonensis*, *H. spadix*, and *H. obscurus*; he wrote "… these species tend to be somewhat more hirsute than the other species … group also lacks the externally visible dorsal telson glands …" These statements agree with the observations presented in this paper, the patellar setation in particular (see our character 32). This subgroup is distributed primarily in the southwestern United States. The third subgroup of Williams (1970b) was comprised of *H. concolorous*, *H. pinteri*, and *H. hirsutus*, distributed exclusively in Baja California peninsula, Mexico; he noted that in "… Two of these [species] … development of a pair … glandular … base of the aculeus …" This statement is consistent with our aculear-gland loss hypothesis.

Later, Soleglad (1976: 117–118) presented a key to all eight species of Hadrurinae based entirely on the trichobothrial patterns of the pedipalp chelae. In this key, groups and subgroups partitioning the taxa were proposed. It is interesting to point out that the key in Soleglad (1976) paralleled the three subgroups suggested by Williams (1970b), who did not use any trichobothrial data, and is also consistent with the cladistic-based phylogeny presented in this paper (Fig. 26).

Geographic distribution of Iuroidea

The geographic distribution of superfamily Iuroidea presents some very interesting disjunctions (Francke & Soleglad, 1981; Sissom & Fet, 2000): Family Iuridae is found in the Old World and family Caraboctonidae, in the New World. Caraboctonidae presents two additional disjunctions: Subfamily Caraboctoninae is distributed in South America and Hadrurinae in North America. Hadrurinae further splits into two parts, the United States and Baja California, Mexico, for genus *Hadrurus*, and southern mainland Mexico for *Hoffmannihadrurus*.

Family Iuridae. Species of this family are found in a relatively small Mediterranean area in southern Greece, Aegean islands, and Turkey. Genus *Calchas* (=*Paraiurus* Francke, 1985) is found primarily in Turkey and the adjacent Greek islands of Megisti (Kastelorizo) (Stathi & Mylonas, 2001) and Samos (Sissom, 1987). *Iurus* is widely distributed in the Greek Peloponnese, Crete, Karpathos and Rhodes Islands, and southern Turkey. For biogeographic considerations, we consider these two genera occupying one area in our model.

Family Caraboctonidae. This family has a disjunct distribution, subfamily **Caraboctoninae** in South America, and Hadrurinae in North America. In Caraboctoninae, the monotypic genus *Caraboctonus* is primarily found in Chile with one record from extreme southern Peru (Lourenço, 1995: fig. 14). The sister genus *Hadruroides*, with nine species, is found throughout Ecuador and Peru, as well as in the Galapagos Islands. For biogeographic considerations these two genera are each assigned different areas.

Subfamily **Hadrurinae** distribution is of primary interest in this discussion. The map shown in Fig. 28 presents the general distribution of its two disjunct genera, *Hoffmannihadrurus* and *Hadrurus*, as well as their eight species. In addition, the map indicates the three phylogenetic subgroups originally defined by Williams (1970b) (as discussed above).

Mainland Mexico. The distribution of the two species of *Hoffmannihadrurus* forms a small disjunction, which may be reduced by further collecting in the area. Presently, *H. gertschi* has only been collected in the state of Guerrero, and *H. aztecus* is primarily found in Puebla and Oaxaca.

We will discuss the distribution of *Hadrurus* species in two groups of ranges: species found primarily in the southwestern United States and those found exclusively in Baja California, Mexico (i.e., second and third subgroups of Williams (1970b)).

United States. Three species are found in the southwestern areas of the United States with some dispersal into the northern areas of Baja California and mainland Mexico. In the United States, subspecies *H. arizonensis arizonensis* is distributed in western Arizona, southern California, and the extreme southern portion of Nevada. The range of *H. a. arizonensis* extends into the extreme western edge of Sonora, Mexico as far south as Guaymas and into northern Baja California. Subspecies *H. a. austrinus* is found further south in Baja California, on the extreme eastern coast of the peninsula, between Oakies Landing and Bahia San Luis Gonzaga (Williams, 1970b: 28). *H. spadix* is found in northern Arizona, southern Utah, the southern and eastern Nevada, extreme east-central California, and the southern areas where states Oregon and Idaho meet. The range of *H. obscurus* is limited to southern California and extends into extreme northern Baja California, Mexico.

Baja California. Three *Hadrurus* species are endemic to the Baja California peninsula and adjacent islands. *H. pinteri* has a disjunct range at the eastern coast of the peninsula (see Fig. 27), occurring in the central portions of Baja California and the north-central portion of Baja California Sur. This disjunct distribution appears to be caused by this species affinity for volcanic microhabitats. Williams (1970b) states: "… species was never found in predominantly sandy habitats or away from habitats of volcanic origin …" *H. pinteri* has also been reported in the Gulf of California from Islas Coronados and Danzante. *H. concolorous* has an extensive range from Bahia de Los Angeles in Baja California to La Paz in Baja California Sur. It is primarily found in sandy habitats although it was also found in volcanic valleys coexisting with *H. pinteri* (Williams, 1970b). Finally, *H. hirsutus* has a very small range limited to the Cape region of Baja California Sur, from Cabo San Lucas to La Paz. Interestingly, the range of this species is limited on the north by the well-studied biogeographic line indicating so-called La Paz Strait (a Pliocene seaway that isolated the Cape) (see e.g. Riddle *et al*., 2000; Riginos, 2007; also compare pilot study of Gantenbein *et al*., 2001, for buthid scorpions *Centruroides*). Phylogenetic reconstructions of historical biogeography for Baja California scorpions are a virtually untouched, and a highly desirable subject.

With respect to our biogeographic model, subfamily Hadrurinae is assigned eleven intersecting areas.

BIOGEOGRAPHIC MODEL

In their cladistic analysis of genus *Hadrurus*, Fet *et al*. (2001) combined biogeographic characters with the morphology-based characters, the approach criticized by Prendini & Wheeler (2005). Here, we utilize biogeographic "characters" (nested areas of distribution) separately to generate an area-based tree that can be compared with the cladogram derived from morphology-based characters.

Above, we briefly described the geographic distribution of superfamily Iuroidea. We represent this distribution, adding that of our morphological outgroup *Chaerilus*, with five characters. Each succeeding character reduces the previous areas as long as the distribution of species in our ingroup can be further refined. When outgroup/ingroup taxa can no longer be refined, they are considered to be "inapplicable" in the characters to follow. Refer to map in Fig. 28 for detailed distribution of subfamily Hadrurinae. The following five characters were analyzed in a PAUP sequence.

Character-a: Worldwide geographic areas (**0:** Southeast Asia [*Chaerilus*]); **1:** Southeastern Europe (Greece) and western Asia (Turkey) [*Iurus*, *Calchas*]; **2:** Western hemisphere [*Caraboctonus*, *Hadruroides*, *Hadrurus*, *Hoffmannihadrurus*]).

Character-b: Western hemisphere (**0:** South America [*Caraboctonus*, *Hadruroides*]; **1:** North America [*Hadrurus*, *Hoffmannihadrurus*]).

Character-c: Regional areas (**0:** Chile area [*Caraboctonus*]; **1:** Peru/Ecuador area [*Hadruroides*]; **2:** United States/Baja California area [*Hadrurus pinteri*, *H. concolorous*, *H. hirsutus*, *H. arizonensis*, *H. spadix*, *H. obscurus*]; **3:** Mexico area, [*Hoffmannihadrurus aztecus*, *H. gertschi*]).

Character-d: Subregional areas (**0:** Baja California area [*Hadrurus pinteri*, *H. concolorous*, *H. hirsutus*]; **1:** United States area [*H. arizonensis*, *H. spadix*, *H. obscurus*]).

Character-e: Microregional areas (**0:** Baja California (northern state)/Baja California Sur-*volcanic* area [*Hadrurus pinteri*]; **1:** Baja California Sur area [*H. concolorous*, *H. hirsutus*]; **2:** California-Arizona area [*H. arizonensis*]; **3:** California-Nevada area [*H. spadix*, *H. obscurus*]).

Result: These five area-characters generated the tree shown in Fig. 25. This tree is based on the majority-rule consensus of 3638 MPTs with the following support: steps/CI/RI/G-fit = 15/1.0/1.0/-5.0. There was no ordering or weighting of these characters. All clades were supported by at least 54 % of the trees. Of particular interest here, and the purpose of this biogeographic model, is to demonstrate that biogeographic distribution of superfamily Iuroidea, with its no less than three major range disjunctions, is *completely congruent*

with the phylogeny derived from our independent cladistic analysis of morphological characters (Figs. 24 and 26). This simplistic model shows disjunctions that could result from vicariant events facilitating speciation and evolution of higher taxa (provided that no significant secondary dispersal/extinction events took place). Further investigation of paleogeographic events in the North American part of iuroid range, combined with further phylogenetic and phylogeographic analysis of *Hadrurus* and *Hoffmannihadrurus*, would undoubtedly add to our knowledge of speciation process in these taxa, as this was recently done for the Mediterranean genus *Iurus* by Parmakelis *et al*. (2006).

Acknowledgements

We thank Anthea Carmichael, Pierangelo Crucitti, Willis J. Gertsch, Matthew R. Graham, Charles Griswold, Jürgen Gruber, František Kovařík, Gary A. Polis, and Darrell Ubick for the loans and/or gifts of specimens. We are grateful to Matthew R. Graham, Graeme Lowe, and Sara Tallarovic for information on *Hadrurus* distribution and biology. Finally, we extend our gratitude to two anonymous reviewers of this paper.

Bibliography

ANDERSON, R. C. 1975. Scorpions of Idaho. *Tebiwa*, **18**(1): 1–17.

BAPTISTA, C., J. A. SANTIAGO-BLAY, M. E. SOLEGLAD & V. FET 2006. The Cretaceous scorpion genus, *Archaeobuthus*, revisited (Scorpiones: Archaeobuthidae). *Euscorpius*, **25**: 1–40.

FRANCKE, O. F. & L. PRENDINI 2008. Phylogeny and classification of the giant hairy scorpions, *Hadrurus* Thorell (Iuridae Thorell): a reappraisal. *Systematics and Biodiversity*, **6**(2): 205–223.

FRANCKE, O. F. & M. E. SOLEGLAD 1981. The family Iuridae Thorell (Arachnida, Scorpiones). *Journal of Arachnology*, **9**: 233–258.

FET, V., M. E. SOLEGLAD 2005. Contributions to scorpion systematics. I. On recent changes in high-level taxonomy. *Euscorpius*, **31**: 1–13.

FET, V., M. E. SOLEGLAD & M. D. BARKER 2001. Phylogenetic analysis of the "*hirsutus*" group of the genus *Hadrurus* Thorell (Scorpiones: Iuridae) based on morphology and mitochondrial DNA. Pp. 139–160 *in* FET, V. & P. A. SELDEN (eds.), *Scorpions 2001. In Memoriam Gary A. Polis.* Burnham Beeches, Bucks: British Arachnological Society.

FET, V., M. E. SOLEGLAD, D. P. A. NEFF & I. STATHI 2004. Tarsal armature in the superfamily Iuroidea (Scorpiones: Iurida). *Revista Ibérica de Aracnología*, **10**: 17–40.

GANTENBEIN, B., V. FET & M. D. BARKER 2001. Mitochondrial DNA markers reveal a deep, divergent phylogeny in *Centruroides exilicauda* (Wood) (Scorpiones: Buthidae). Pp. 235–244 *in* FET, V. & P. A. SELDEN (eds.), *Scorpions 2001. In memoriam Gary A. Polis.* Burnham Beeches, Bucks: British Arachnological Society.

GERTSCH, W. J. & D. M. ALLRED 1965. Scorpions of the Nevada Test Site. *Brigham Young University Science Bulletin, Biological Series*, **6**(4): 1–15.

GOLOBOFF, P. A. 1993. Estimating character weights during tree search. *Cladistics*, **9**: 83–91.

HOFFMANN, C. C. 1931. Monografias para la entomología médica de México. Monografia Num. 2, Los escorpiones de México. Primera parte: Diplocentridae, Chactidae, Vejovidae. *Anales del Instituto de Biología, Universidad Nacional Autónoma de México*, **2**(4): 291–408.

KITCHING, I. J., P. L. FOREY, C. J. HUMPHRIES & D. WILLIAMS 1998. *Cladistics: Theory and Practice of Parsimony Analysis*. 2nd Ed. Oxford University Press: London, 242 pp.

JOHNSON, J. D. & D. M. ALLRED 1972. Scorpions of Utah. *Great Basin Naturalist*, **32**(3): 154–170.

LOURENÇO, W. R. 1995. Considérations sur la morphologie, écologie et biogéographie de *Caraboctonus keyserlingi* Pocock (Scorpiones, Iuridae). *Boletín de la Sociedad Biológica de Concepción*, **66**: 63–69.

MACKAY, T. F. C. 1996. The nature of quantitative genetic variation revisited: lessons from *Drosophila* bristles. *Bioessays*, **18**: 113–121.

MACKAY, T. F. C. 2001. The genetic architecture of quantitative traits: Inferences from *Drosophila* sensory bristle number. Pp. 389–409 *in* WAGNER, G. P. (ed), *The Character Concept in Evolutionary Biology*, edited by Academic Press, San Diego, CA.

NIXON, K. C. 1999. *Winclada. Beta Version 0.9.99i*. Ithaca, New York: Published by the Author.

PAGE, R. D. M. 1998. *TreeView (win32) 1.5.2*. Glasgow, Scotland.

PARMAKELIS, A., I. STATHI, L. SPANOS, C. LOUIS & M. MYLONAS 2006. Phylogeography of *Iurus dufoureius* (Brullé, 1832) (Scorpiones, Iuridae). *Journal of Biogeography*, **33**(2): 251–260.

PRENDINI, L. 2000. Phylogeny and classification of the superfamily Scorpionoidea Latreille 1802 (Chelicerata, Scorpiones): An exemplar approach. *Cladistics*, **16**: 1–78.

PRENDINI, L. 2003. A new genus and species of bothriurid scorpion from the Brandberg Massif, Namibia, with a reanalysis of bothriurid phylogeny and a discussion of the phylogenetic position of *Lisposoma* Lawrence. *Systematic Entomology*, **28**: 149–172.

PRENDINI, L. & W. C. WHEELER 2005. Scorpion higher phylogeny and classification, taxonomic anarchy, and standards for peer review in online publishing. *Cladistics*, **21**: 446–494.

RIDDLE, B., D. J. HAFNER, L. F. ALEXANDER & J. R. JAEGER 2000. Cryptic vicariance in the historical assembly of a Baja California Peninsular Desert biota. *Proceedings of the National Academy of Science USA*, 97(26): 14438–14443

RIGINOS, C. 2007. Cryptic vicariance in Gulf of California fishes parallels vicariant patterns found in Baja California mammals and reptiles. *Evolution* **59**(12): **2**678–2690.

SISSOM, W. D. 1987. First record of the scorpion *Paraiurus nordmanni* (Birula, 1899) (Scorpiones, Iuridae) in Greece. *Journal of Arachnology* **15**: 272.

SISSOM, W. D. & V. FET 2000. Family Iuridae Thorell, 1876. Pp. 409–420 *in* Fet, V., W. D. Sissom, G. Lowe & M. E. Braunwalder. *Catalog of the Scorpions of the World* (1758–1998). New York, NY: New York Entomological Society, 690 pp.

SOLEGLAD, M. E. 1976. The taxonomy of the genus *Hadrurus* based on chela trichobothria (Scorpionida: Vejovidae). *Journal of Arachnology*, **3**: 113–134.

SOLEGLAD, M. E. & V. FET 2001. Evolution of scorpion orthobothriotaxy: a cladistic approach. *Euscorpius*, **1**: 1–38.

SOLEGLAD, M. E. & V. FET 2003a. The scorpion sternum: structure and phylogeny (Scorpiones: Orthosterni) *Euscorpius*, **5**: 1–34.

SOLEGLAD, M. E. & V. FET 2003b. High-level systematics and phylogeny of the extant scorpions (Scorpiones: Orthosterni). *Euscorpius*, **11**: 1–175.

SOLEGLAD, M. E. & V. FET 2006. Contributions to scorpion systematics. II. Stahnkeini, a new tribe in scorpion family Vaejovidae (Scorpiones: Chactoidea). *Euscorpius*, **40**: 1–32.

SOLEGLAD, M. E., V. FET & F. KOVAŘÍK 2005. The systematic position of the scorpion genera *Heteroscorpion* Birula, 1903 and *Urodacus* Peters, 1861 (Scorpiones: Scorpionoidea). *Euscorpius*, **20**: 1–38.

SOLEGLAD, M. E. & W.D. SISSOM 2001. Phylogeny of the family Euscorpiidae Laurie, 1896: a major revision. Pp. 25–111 *in* V. Fet & P. A. Selden (eds.). *Scorpions 2001. In Memoriam Gary A. Polis*. Burnham Beeches, Bucks: British Arachnological Society.

STAHNKE, H. L. 1945. Scorpions of the genus *Hadrurus*. *American Museum Novitates*, **1298**: 1–9.

STAHNKE, H. L. 1969. Review of *Hadrurus* scorpions (Vejovidae). *Entomological News*, **80**(3): 57–65.

STAHNKE, H. L. 1971. The redescription of the scorpion, *Hadrurus aztecus* (Vejovidae). *Entomological News*, **82**: 121–131.

STOCKWELL, S. A. 1989. *Revision of the Phylogeny and Higher Classification of Scorpions (Chelicerata).* Ph.D. Dissertation, University of Berkeley, Berkeley, California. 319 pp. (unpublished). University Microfilms International, Ann Arbor, Michigan.

SWOFFORD, D. L. 1998. *PAUP* Phylogenetic Analysis Using Parsimony (*and Other Methods)*. Version 4. Sinauer Associates: Sunderland, Massachusetts.

VACHON, M. 1963. De l'utilité, en systématique, d'une nomenclature des dents de chelicères chez les Scorpions. *Bulletin du Muséum National d'Histoire Naturelle, Paris*, (2), **35**(2): 161–166.

VACHON, M. 1971. [Remarques sur le Scorpion caucasien *Calchas nordmanni* Birula (Scorpiones, Chactidae)]. *Entomologicheskoe Obozrenie (Revue d'Entomologie de l'URSS)*, **50**(3): 712–718 (in Russian). English translation: *Entomological Review*, **50**(3): 712–718.

VACHON, M. 1974. Étude des caractères utilisés pour classer les familles et les genres de Scorpions (Arachnides). 1. La trichobothriotaxie en Arachnologie. Sigles trichobothriaux et types de trichobothriotaxie chez les Scorpions. *Bulletin du Muséum National d'Histoire Naturelle, Paris,* (3), mai-juin 1973, **140** (Zool. 104): 857–958.

WILLIAMS, S. C. 1970a. A redescription of *Hadrurus pinteri* Stahnke based on the adult (Scorpionida: Vejovidae). *The Wasmann Journal of Biology*, **28**(1): 169–174.

WILLIAMS, S. C. 1970b. A systematic revision of the giant hairy scorpion genus *Hadrurus*. *Occasional Papers of the California Academy of Sciences*, **87**: 1–62.

WILLIAMS, S. C. 1980. Scorpions of Baja California, Mexico and adjacent islands. *Occasional Papers of the California Academy of Sciences*, **135**: 1-127.